

Isolation and Characterization of High-Temperature-Induced Dauer Formation Mutants in *Caenorhabditis elegans*

Michael Ailion* and James H. Thomas*^{*,†,1}

*Molecular and Cellular Biology Program of the University of Washington and Fred Hutchinson Cancer Research Center and
†Department of Genome Sciences, University of Washington, Seattle, Washington 98195

Manuscript received January 9, 2002
Accepted for publication April 3, 2003

ABSTRACT

Dauer formation in *Caenorhabditis elegans* is regulated by at least three signaling pathways, including an insulin receptor-signaling pathway. These pathways were defined by mutants that form dauers constitutively (Daf-c) at 25°. Screens for Daf-c mutants at 25° have probably been saturated, but failed to identify all the components involved in regulating dauer formation. Here we screen for Daf-c mutants at 27°, a more strongly dauer-inducing condition. Mutations identified include novel classes of alleles for three known genes and alleles defining at least seven new genes, *hid-1*–*hid-7*. Many of the genes appear to act in the insulin branch of the dauer pathway, including *pdk-1*, *akt-1*, *aex-6*, and *hid-1*. We also molecularly identify *hid-1* and show that it encodes a novel highly conserved putative transmembrane protein expressed in neurons.

WHEN exposed to environmental conditions unfavorable for growth and reproduction, the nematode *Caenorhabditis elegans* forms arrested third stage larvae called dauers (CASSADA and RUSSELL 1975; RIDDLER and ALBERT 1997). Entry into the dauer stage is regulated by at least three environmental signals: temperature, food availability, and the concentration of a pheromone that serves as an indicator of population density (GOLDEN and RIDDLER 1984a,b,c). It is likely that internal metabolic signals also regulate dauer formation (KIMURA *et al.* 1997).

Extensive genetic analysis of dauer formation has led to the isolation of many mutants that fall into two general classes: dauer formation constitutive (Daf-c) mutants, which form dauers inappropriately under noninducing conditions, and dauer formation defective (Daf-d) mutants, which fail to form dauers under inducing conditions. These mutants define at least three branches of a complicated genetic pathway (VOWELS and THOMAS 1992; THOMAS *et al.* 1993; GOTTLIEB and RUVKUN 1994). The group I branch regulates cyclic GMP signaling in sensory neurons that respond to pheromone (BIRNBY *et al.* 2000). The group II branch consists of components of a TGF- β signaling pathway; release of a TGF- β -like ligand from sensory neurons leads to activation of receptors and downstream pathways in target cells (GEORGI *et al.* 1990; ESTEVEZ *et al.* 1993; REN *et al.* 1996; SCHACKWITZ *et al.* 1996; PATTERSON *et al.* 1997; INOUE and

THOMAS 2000a). The third branch of the pathway consists of components of an insulin receptor-signaling pathway (MORRIS *et al.* 1996; KIMURA *et al.* 1997; LIN *et al.* 1997; OGG *et al.* 1997; PARADIS and RUVKUN 1998; PARADIS *et al.* 1999). The genes of this pathway appear to function in several different tissues (APFELD and KENYON 1998; WOLKOW *et al.* 2000).

Screens for simple loss-of-function mutants with a strong Daf-c phenotype at 25° have probably been saturated (*e.g.*, MALONE and THOMAS 1994), defining the genes found in the three branches described above. However, on the basis of biochemical expectations, there should be other components of these pathways. For example, the insulin pathway consists of only two Daf-c genes found at 25°: *daf-2*, the insulin receptor, and *age-1*, a phosphatidylinositol-3-OH kinase (PI3K) that is a direct target of the insulin receptor. Signaling components downstream of *age-1* were expected, but not identified. The existence of more Daf-c genes is also supported by the discovery of synthetic Daf-c (Syn-Daf) mutants in which the single mutants are not Daf-c at 25°, but the double mutant is Daf-c. Genes belonging to this class include *unc-64*, *unc-31*, *unc-3*, *aex-3*, *egl-4*, *flr-1*, *flr-3*, *flr-4*, *tph-1*, and the *dyf* genes (AVERY 1993; KATSURA *et al.* 1994; IWASAKI *et al.* 1997; TAKE-UCHI *et al.* 1998; AILION *et al.* 1999; AILION and THOMAS 2000; DANIELS *et al.* 2000; SZE *et al.* 2000). All of these mutants were originally identified on the basis of other phenotypes, such as uncoordinated locomotion (Unc), defective egg laying (Egl), defective defecation (Aex), or fluoride resistance (Flr). Such mutants would not have been isolated in the many previous screens for Daf-c mutants at 25°. The Syn-Daf phenotype was discovered only accidentally in the course of studying the mutants

Sequence data from this article have been deposited with the EMBL/GenBank Data Libraries under accession no. AY070228.

¹Corresponding author: Department of Genome Sciences, University of Washington, Box 357730, Seattle, WA 98195.
E-mail: jht@u.washington.edu

for other reasons. Thus, there could be many unidentified mutants with a Syn-Daf phenotype, especially mutants that do not have other pleiotropic phenotypes.

Unfortunately, screening directly for mutants on the basis of a synthetic phenotype is difficult because two independent mutations are required to generate the phenotype. The finding that many of the Syn-Daf genes have strong single mutant Daf-c phenotypes at 27° (AILION and THOMAS 2000; DANIELS *et al.* 2000) provides for an alternative way to identify such dauer genes. Here we describe the results of performing a screen for Daf-c mutants at 27°, a phenotype that we call Hid (for high-temperature-induced dauer formation). The large number of mutants precluded a complete genetic analysis. From the subset of mutants we selected for more thorough analysis, several new dauer genes were identified. On the basis of their gene interactions, many of the mutants appear to have defects in the insulin branch of the dauer pathway, a branch in which few Daf-c genes had been identified previously. We also molecularly identified *hid-1*, one of the new genes in the insulin branch, and show that it encodes a novel highly conserved protein with many potential transmembrane domains.

MATERIALS AND METHODS

General growth conditions: All *C. elegans* strains were derivatives of the wild-type strain N2 and were cultured using standard methods (BRENNER 1974; AILION and THOMAS 2000). Growth at 27° requires special care and was performed as described (AILION and THOMAS 2000).

Assay reproducibility and reporting: Dauer formation at temperatures above 25° is very sensitive to small temperature differences, both in the wild type and in various mutants. Our best efforts to control incubator temperature were insufficient to prevent significant variability in dauer counts. These issues are described in considerable detail in an earlier article (AILION and THOMAS 2000) and summarized here. Data presented in each block in tables are from a single set of assays that were conducted at the same time on the same incubator shelf. Under these conditions, relative dauer formation frequencies among different strains are consistent (*e.g.*, if strain A > strain B in one set of assays, the same relation will hold in other assays) whereas absolute dauer formation frequencies differ (strain A varies from assay to assay). The “temperature” reported is the average of the temperature on the assay shelf when the assay began and when it ended. All assays were repeated at least three times and the relative dauer formation among all comparable strains in each assay was similar, though the absolute levels varied. We refer to a Hid phenotype as “strong” if >90% of animals consistently form dauers at 27°, “moderate” if 70–90% dauers are formed, and “weak” if <70% dauers are formed. Because of temperature deviation from 27° in individual assays, reported numbers may not conform to these values perfectly.

Survey of preexisting mutants for a Daf-c phenotype at 27°: The following mutants were grown at 27° and examined for a Daf-c phenotype: *aex-1(sa9)*, *aex-2(sa3)*, *aex-3(ad418)*, *aex-3(y255)*, *aex-4(sa22)*, *aex-5(sa23)*, *aex-6(sa24)*, *akt-1(mg144gf)*, *bli-1(e769)*, *cam-1(ks52)*, *cat-4(e1141)*, *cha-1(p1152)*, *che-14(e1960)*, *clk-1(e2519)*, *deg-3(u662gf)*, *dpy-3(e27)*, *dpy-4(e1166)*, *dpy-5(e61)*, *dpy-6(e14)*,

dpy-9(e12), *dpy-10(e128)*, *dpy-11(e224)*, *dpy-17(e164)*, *dpy-18(e364)*, *dpy-20(e1282)*, *eat-1(ad427)*, *eat-4(ad572)*, *eat-6(ad467)*, *egl-2(n693gf)*, *egl-3(n150)*, *egl-9(sa307)*, *egl-10(n692)*, *egl-10(md176)*, *nIs51[egl-10 XS]*, *egl-19(n582)*, *egl-19(ad695gf)*, *egl-19(n2368gf)*, *egl-21(n576)*, *egl-32(n155)*, *egl-36(n2332gf)*, *egl-40(n606)*, *egl-46(n1075)*, *exp-1(sa6)*, *exp-4(n2373gf)*, *flp-1(yn2)*, *flp-1(yn4)*, *ynIs9[hsp16-2::flp-1]*, *flr-4(sa201)*, *goa-1(n1134)*, *syIs9[goa-1(act)]*, *gpa-1(pk15)*, *pkIs503[gpa-1 XS]*, *gpa-2(pk16)*, *syIs13[gpa-2(act)]*, *gpa-3(pk35)*, *syIs24[gpa-3(act)]*, *gpa-4(pk381)*, *pkIs515[gpa-4 XS]*, *gpa-5(pk376)*, *pkIs379[gpa-5 XS]*, *gpa-6(pk480)*, *pkIs519[gpa-6 XS]*, *gpa-7(pk610)*, *pkIs523[gpa-7 XS]*, *gpa-8(pk345)*, *pkIs527[gpa-8 XS]*, *gpa-9(pk438)*, *gpa-10(pk362)*, *pkIs533[gpa-10 XS]*, *gpa-11(pk349)*, *pkIs539[gpa-11 XS]*, *gpa-13(pk1270)*, *gpa-14(pk347)*, *gpa-15(pk477)*, *lin-2(e1309)*, *lin-10(e1438)*, *lin-11(n566)*, *lin-32(u282)*, *lon-2(e678)*, *lon-2(n1630)*, *npr-1(ad609)*, *odr-1(n1936)*, *odr-2(n2145)*, *odr-3(n1605)*, *odr-4(n2144)*, *odr-5(ky9)*, *odr-6(ky1)*, *osm-9(n1601)*, *osm-10(n1602)*, *pbo-1(sa7)*, *pdk-1(mg142gf)*, *rol-1(e91)*, *rol-3(e754)*, *rol-6(e187)*, *scd-1(sa248)*, *scd-3(sa253)*, *sma-1(e30)*, *sma-2(e502)*, *sma-3(e491)*, *sma-4(e729)*, *snb-1(md247)*, *snt-1(md125)*, *spe-26(hc138)*, *srd-1(eh1)*, *tph-1(mg280)*, *ttx-1(p767)*, *unc-1(e580)*, *unc-1(e719)*, *unc-2(e55)*, *unc-4(e120)*, *unc-5(e53)*, *unc-7(e5)*, *unc-9(e101)*, *unc-11(e47)*, *unc-13(e51)*, *unc-13(e450)*, *unc-13(e1091)*, *unc-16(e109)*, *unc-17(e113)*, *unc-18(e81)*, *unc-24(e138)*, *unc-25(e156)*, *unc-29(e193)*, *unc-29(e1072)*, *unc-32(e189)*, *unc-33(e204)*, *unc-36(e251)*, *unc-38(e264)*, *unc-38(x411)*, *unc-41(e268)*, *unc-42(e270)*, *unc-43(e266)*, *unc-43(sa200)*, *unc-43(n498gf)*, *unc-44(e1197)*, *unc-46(e177)*, *unc-47(e307)*, *unc-49(e382)*, *unc-58(e665gf)*, *unc-58(e757gf)*, *unc-58(e1320gf)*, *unc-58(n495gf)*, *unc-58(e415gf)*, *unc-63(x37)*, *unc-65(e351)*, *unc-70(n493gf)*, *unc-70(e524gf)*, *unc-75(e950)*, *unc-76(e911)*, *unc-86(n846)*, *unc-95(su33)*, *unc-100(su115)*, *unc-101(m1)*, *unc-101(sy108)*, *unc-101(rh6)*, *unc-103(e1597gf)*, *unc-103(n500gf)*, *unc-104(e1265)*, *unc-119(e2498)*, *vab-8(e1017)*, *scd(sa315)*, *sa615*, and the double mutants *egl-17(e1313)* *lon-2(n1442)*, *gpa-2(pk16)* *gpa-3(pk35)*, and *unc-5(e53)* *lin-45(n2018)*.

At 27°, some mutants grew slowly and often arrested as larvae and, hence, were difficult to assay for a Hid phenotype. These included *cha-1*, *che-14*, *eat-1*, *pbo-1*, *sma-4*, *snt-1*, *unc-11*, *unc-18*, *unc-70*, *unc-104*, and *sa615*. Some animals from all except *sma-4* grew past the dauer stage and were not obviously Hid. Some strains had a Hid phenotype that could be accounted for by a background mutation present in the strain. The JT6 *exp-1(sa6)* and CB120 *unc-4(e120)* strains had strong Hid phenotypes, but in both cases the Hid phenotype was due to the presence of a weak *daf-2* mutation in the strain background (now named *sa753* in JT6 and *sa875* in CB120). The Hid phenotype of the CB138 *unc-24(e138)* strain was due to a background mutation in the *tax-2* gene (see RESULTS). *unc-13(e450)* was Hid and Dyf, but *unc-13(e51)* and *unc-13(e1091)* were not. Many *daf* mutants are Hid (AILION and THOMAS 2000). The *daf* mutation in the CB450 *unc-13(e450)* strain (now named *sa1272*) was closely linked to *unc-13* and was shown to be allelic to *che-3*.

Other Hid phenotypes that were probably due to a Dyf phenotype were those of *flp-1(yn2)*, *yn4*, *unc-101(m1)*, *sy108*, and *unc-119(e2498)*. Strains bearing *unc-101(m1)*, *unc-101(sy108)*, and *unc-119(e2498)* were Hid and Dyf, but *unc-101(rh6)* was neither Hid nor Dyf. We did not determine whether or not these Dyf phenotypes are from linked *daf* gene mutations. *flp-1(yn2)* and *flp-1(yn4)* both were Dyf. We found that *flp-1(yn2)* failed to complement *daf-10(e1387)* for the Dyf phenotype, indicating that the *flp-1* mutant strain also carries a mutation in *daf-10*. *daf-10* is encoded by F23B2.4 (S. STONE and J. SHAW, personal communication; QIN *et al.* 2001), the gene immediately upstream of *flp-1*. Further inspection of the *flp-1* deletion mutations indicates that both *yn2* and *yn4* delete the *daf-10* promoter and from two to four exons of the predicted *daf-10* coding sequence. The original Tc1 transposon insertion used to isolate the *flp-1* deletions appears to reside in the *daf-10*

gene (NELSON *et al.* 1998), and both *flp-1* deletion alleles are likely null for both genes. There are no mutations that specifically disrupt *flp-1*, so its effects on dauer formation could not be tested. Disruption of the *daf-10* gene is probably responsible for several of the reported *flp-1* mutant phenotypes (NELSON *et al.* 1998).

Mutant strains that had significant Hid phenotypes that could not be accounted for by background mutations or a Dyf phenotype were *aex-3(ad418)*, *aex-3(y255)*, *cam-1(ks52)*, *syIs13[gpa-2(act)]*, *syIs24[gpa-3(act)]*, *pkIs539[gpa-11 XS]*, *tph-1(mg280)*, *unc-43(n498)*, and the *unc-58* strains. The Hid phenotypes of *aex-3* and *unc-43(n498)* were relatively weak. Both of these genes have Syn-Daf phenotypes in certain combinations (*aex-3* with *unc-31* or *unc-64*, *unc-43(n498)* with *tax-4* or *osm-6*). *unc-58(e665)*, *unc-58(e757)*, *unc-58(e1320)*, and *unc-58(n495)* had a strong Hid phenotype. *unc-58(e415)* has a weaker Unc phenotype and also has only a weak Hid phenotype. *unc-58* has been reported as having defects in dauer recovery (MALONE *et al.* 1996). *syIs13[gpa-2(act)]* and *syIs24[gpa-3(act)]* were previously reported as having Daf-c phenotypes at lower temperatures (ZWAAL *et al.* 1997). *tph-1(mg280)*, which is deficient in serotonin biosynthesis, was reported as having a very weak Daf-c phenotype at temperatures between 15° and 25° (DANIELS *et al.* 2000; SZE *et al.* 2000). It has a much stronger Daf-c phenotype at 27° [e.g., in one experiment, *tph-1* formed 69% dauers, N2 formed 2%, and *unc-31(e928)* formed 99%]. *cam-1(ks52)* had a strong Hid phenotype, as discussed in RESULTS. Other mutants with weaker or variable Hid phenotypes were *aex-4*, *lin-32*, *lon-2*, *unc-7*, *unc-9*, *unc-16*, and *unc-32*. It is possible that an apparent weak Hid phenotype could simply be due to a slower growth rate than that of N2 or to slower recovery of dauers.

Screen for Daf-c mutants in an *aex-3* background: To measure the efficacy of screening for synthetic Daf-c mutants in the background of a Syn-Daf single mutant, we performed a moderately sized F₂ screen (5800 EMS-mutagenized haploid genomes) for Daf-c mutants at 25° in the *aex-3(ad418)* mutant background. We isolated 14 independent mutants. For all but 1, the Daf-c phenotype did not depend on the *aex-3* mutation, indicating that the mutants were not synthetic. The 1 Syn-Daf mutant isolated was an allele of *unc-31*, already known to be Syn-Daf with *aex-3*. The other 13 mutants were new alleles of previously known Daf-c genes: two *daf-1*, three *daf-2*, five *daf-8*, two *daf-11*, and one *tax-4*. Since only 1 of 14 mutants isolated was Syn-Daf, probably few genes can be mutated to give a strong Syn-Daf phenotype in combination with *aex-3*.

Screen for Daf-c mutants at 27°: EMS mutagenesis of N2 was performed as described (BRENNER 1974). Semisynchronous F₁ broods of mutagenized parents were grown at 20° to the young adult stage and then shifted to 27°. The F₂ generation was screened for dauers at appropriate times. Dauers were picked to plates at 15° and allowed to recover. Depending on the precise time of screening, we may have biased our screen for dauers that fail to recover rapidly at 27°. Since N2 forms dauers transiently at a low frequency at 27° (AILION and THOMAS 2000), we attempted to enrich for mutants by screening plates at a time point when most of the N2 dauers had recovered. Nevertheless, many putative mutants failed to retest as Daf-c at 27°, indicating that the screen had a significant background of false positives. Mutants with a Daf-c phenotype significantly stronger than N2 were kept. All but one of the mutants isolated came from the EMS screens of ~13,000 mutagenized haploid genomes. The last mutant [*daf-8(sa829)*] came from a single round (400 genomes) of X-ray mutagenesis using 3500 rads. *daf-8(sa829)* has an unusually strong Daf-c phenotype for *daf-8* mutants.

Behavioral assays: All mutants were outcrossed at least twice before being tested in the behavioral assays reported in the

tables and figures of this article, except as noted. Initial dye filling and pheromone assays were performed on unoutcrossed mutants to decide whether to pursue them further. Dauer formation assays at 27° and on pheromone plates were performed as described (VOWELS and THOMAS 1994; AILION and THOMAS 2000). FITC dye-filling assays were performed as described (HEDGECOCK *et al.* 1985). In some cases, dye filling was also assayed using DiI. Defecation behavior was assayed as described (THOMAS 1990).

Mapping: Mutants were mapped first to a chromosome using standard methods. Mutants with strong Hid phenotypes could be mapped by picking individual parents to 27° and examining their broods for segregation of dauers, which were picked to 15° for recovery and examined for segregation of markers. Since the wild type variably forms some dauers near 27°, it was important to perform control crosses in parallel to mapping crosses. Even with this precaution, potentially misleading mapping results were frequently a problem with weaker Hid mutants and especially mutants that recovered rapidly from the dauer stage. For mutants with weaker phenotypes, we reduced these problems by synchronized egg lays at room temperature followed by a shift to 27°. Even by this method, many mutants were too weak or variable to map efficiently and, if one or two efforts failed, we put such mutants aside.

After a mutation was mapped to a chromosome, the mapping problem became simpler. Standard three-factor mapping was done, in which we did not need to pick individual animals on the basis of their Hid phenotype. Recombinants were homozygosed and the resulting strains were examined as a population at 27° for the Hid phenotype. In cases where marker mutations obscured the Hid phenotype, each recombinant was crossed to homozygous Hid mutant males and scored for Hid cross-progeny.

We mapped *hid-1(sa691)* between *lin-32* and *unc-2* by picking Unc non-Dpy recombinants from *hid-1/dpy-3 lin-32 unc-2* parents. After recombinants were homozygosed, we crossed them to *hid-1* males. Male progeny from these crosses were scored for missing rays to determine the *lin-32* genotype of each recombinant (ZHAO and EMMONS 1995). The presence of *hid-1* was scored in the hermaphrodite progeny of the same cross by either the Hid (at 27°) or the Unc, Con (at 20°) phenotypes.

hid-3 was generally mapped by its Hid phenotype. Recombinants were sometimes rechecked for pheromone responsiveness (Phe phenotype). Several crosses gave results that were inconsistent or anomalous. From the *hid-3/dpy-5 unc-13* cross, all of the Unc non-Dpy recombinants lacked *hid-3*, as scored by either Hid or Phe phenotypes. One Dpy non-Unc recombinant lacked *hid-3*, as scored by Hid phenotype. However, this recombinant appeared to carry *hid-3* as scored by the Phe phenotype. If this one recombinant lacked *hid-3*, it would place *hid-3* to the left of *unc-13*. To further define the position of *hid-3* relative to *unc-13*, we performed two additional crosses. All recombinants from *hid-3/dpy-14 unc-13* placed *hid-3* to the right of or close to *unc-13*. From *hid-3/unc-13 lin-10*, we isolated six Lin non-Unc recombinants. Three of these were Hid and responsive to pheromone [Phe(+)]. The other three were non-Hid and were insensitive to pheromone [Phe(-)]. *hid-3* is Hid and Phe(-) while wild type is non-Hid and Phe(+). Since the Hid and Phe phenotypes of *hid-3* did not cosegregate in these recombinants, it is possible that they are due to two different mutations. However, if the two mutations were linked (as appears extremely likely from all other work on this mutant), we cannot explain both classes of Lin non-Unc recombinants.

Rescuing and sequencing *sa573* and *sa700*: We obtained *mgEx338*, an extrachromosomal array carrying a functional *akt-1::gfp* fusion with *rol-6(d)* as a marker (PARADIS and RUVKUN

1998). We built an *sa573; mgEx338* double mutant to test for rescue. Because we saw significant rescue of the Hid phenotype, we sequenced all *akt-1* exons in the *sa573* mutant by direct sequencing of PCR products amplified from *sa573* worms. For *sa700*, all exons except the first were sequenced.

Rescuing *sa692*: *sa692* animals were injected with a genomic *cam-1(+)* clone (pK8-22.3) at 30 ng/ μ l, *myo-2::gfp* at 5 ng/ μ l, and pBluescript at 78 ng/ μ l as carrier DNA. Transgenic lines were selected by picking animals expressing green fluorescent protein (GFP) in the pharynx, using a dissecting scope equipped with a UV attachment.

***hid-1* noncomplementation screen:** To isolate additional alleles of *hid-1*, we mutagenized N2 males with EMS and crossed them to *dpy-3(e27) hid-1(sa691)* hermaphrodites, screening the F₁ progeny for non-Dpy Unc Con animals at 22° or non-Dpy dauers at 27°. From a screen of ~18,000 mutagenized haploid genomes, we found two new *hid-1* alleles. *sa1056* was picked on the basis of the Unc, Con phenotypes and *sa1058* was picked on the basis of the Hid phenotype.

Rescuing and sequencing *hid-1* mutants: On the basis of the mapping of *hid-1* between the physical markers *lin-32* and *unc-2*, we tested cosmids in the region for transgenic rescue of *hid-1* mutant phenotypes. *hid-1(sa691) lin-15(n765)* animals were injected with candidate cosmids or subclones at 10 ng/ μ l each and pBLH98 [*lin-15(+)*] as the transformation marker at 90 ng/ μ l (MELLO *et al.* 1991; HUANG *et al.* 1994). Transgenic lines were established by picking non-Lin animals at 22° and scored for rescue of the Unc, Con, and Hid phenotypes. Rescue data were as follows (given as the fraction of lines rescuing): cosmid pool C16F4, K08H6, R04B3, K02E10, and C54A10 (9/16 lines rescued); cosmid C16F4 (0/6); cosmid K08H6 (0/8); cosmid R04B3 (0/7); cosmid K02E10 (7/9); cosmid C54A10 (0/5); pTJ1348 (0/7); pTJ1350 (0/2); pTJ1351 (0/13); and pTJ1353 (4/5). Various subclones of K02E10 were made by standard methods. The rescuing subclone pTJ1353 contained an 8.6-kb *XhoI-BamHI* fragment of K02E10, which has a single predicted gene (K02E10.2). All other predicted genes from K02E10 were carried on one or more nonrescuing subclones. All *hid-1* exons and splice junctions were sequenced in the four *hid-1* mutant strains by direct sequencing of PCR products amplified from mutant worms. All mutations were sequenced on both strands from at least two independent PCR products.

Analysis of *hid-1* cDNAs: Three *hid-1* cDNAs that appeared to be close to full length were obtained from Yuji Kohara. A putative *trans*-splice site is found at nucleotide 12044 of cosmid K02E10. The 5' end of each cDNA was sequenced. yk32f11 ended at bp 12073, yk229f10 ended at bp 12047, and yk426f3 ended at bp 12051, all three upstream of the first exon and close to the putative *trans*-splice site. yk32f11 was sequenced completely and has the same gene structure predicted on the National Center for Biotechnology Information database (Figure 3A). Restriction digests of yk229f10 and yk426f3 suggested the same gene structure, and this was confirmed for the first five exons by sequencing. Several additional *hid-1* expressed sequence tags (ESTs) reported in public datasets all have structures consistent with a single splice pattern.

Construction of *hid-1::gfp* fusions: A 5-kb *SphI-BglII* fragment of K02E10 was cloned in two pieces into the *SphI/BamHI* sites of GFP vectors pPD95.67 and pPD95.75 (A. FIRE, S. XU, J. AHNN and G. SEYDOUX, personal communication), with or without a nuclear localization signal (NLS). The resulting constructs carry 4.3 kb of *hid-1* promoter and *gfp* fused in frame in exon 3, leading to a GFP fusion protein at amino acid D134 of HID-1. Constructs were injected into *lin-15(n765)* worms at 25 ng/ μ l with pBLH98 [*lin-15(+)*] as the transformation marker at 90 ng/ μ l and transgenic lines were established by picking non-Lin animals at 22°. Faint expression was seen

in lines with the construct carrying an NLS, but no expression was seen in lines carrying the construct without an NLS, even when it was injected at 125 ng/ μ l.

RESULTS

Survey of existing mutants for dauer formation at 27°: In addition to screening directly for Daf-c mutants at 27° (see below), we assayed a large number of *C. elegans* behavioral and morphological mutants for a Daf-c phenotype at 27°. The list of mutants examined is presented in MATERIALS AND METHODS and includes genes involved in synaptic transmission, neuronal specification or differentiation, axon guidance, odorant response, ion channels, G proteins, neuropeptides, and neurotransmitters. Very few mutants had a strong Hid phenotype, indicating that this phenotype is not commonly caused by general defects in nervous system development or function. For several cases in which a mutant strain exhibited a Hid phenotype, we determined that this phenotype resulted from a background Hid mutation rather than from the mutation being tested (see MATERIALS AND METHODS). Thus, the isolation of mutations with nonspecific effects on dauer formation was not expected to be a major problem confounding a screen for Hid mutants.

Isolation and preliminary characterization of high-temperature-induced dauer formation (Hid) mutants: We screened ~13,000 mutagenized haploid genomes and isolated 103 mutants (*sa533-536*, *sa551-556*, *sa569-574*, *sa645-702*, *sa705-731*, *sa829*, and one mutant subsequently lost). Not all of these were independent, although possible repeat isolates were kept only if they exhibited some phenotypic difference. In three cases we later found that we had isolated the same mutation twice (*sa652* is allelic to *sa709*; *sa697* is allelic to *sa731*; *sa687* is allelic to *sa725*). Since a few other such cases are likely, the number of distinct mutations isolated is probably in the range of 95–100.

We expected to find several classes of mutants that were not our primary interest. First, we expected to isolate mutations in the previously described Daf-c genes that have strong Daf-c phenotypes at 25°. At 25°, 10 of our Hid mutants had a strong Daf-c phenotype. Nine of these are new alleles of previously known Daf-c genes: four *daf-1*, one *daf-2*, one *daf-7*, two *daf-8*, and one *daf-14* (Table 1). The 10th mutation (*sa680*) identified a new gene, *pdk-1*, which has been described elsewhere (PARADIS *et al.* 1999). Second, we expected to isolate mutations in the large group of Dyf genes that cause defects in the structure of the sensory neuron endings and cause a Hid phenotype (AILION and THOMAS 2000). All our mutants were tested for a Dyf phenotype. Five mutants (*sa551*, *sa554*, *sa555*, *sa660*, and *sa682*) had a strong Dyf phenotype (no observed filling of amphid or phasmid neurons by FITC). Since there are many Dyf genes (probably at least 40; STARICH *et al.* 1995),

TABLE 1
Summary of mutants isolated in Daf-c screen at 27°

Gene	Alleles
<i>daf-1</i> IVL	<i>sa536, sa645, sa653, sa678</i>
<i>daf-2</i> IIIIL	<i>sa552*, sa647*, sa651, sa667*, sa672*, sa677*, sa723*, sa728*</i>
<i>daf-7</i> IIIIL	<i>sa533, sa695*</i>
<i>daf-8</i> IC	<i>sa553*, sa669*, sa686, sa690*, sa829</i>
<i>daf-14</i> IVC	<i>sa535</i>
<i>age-1</i> IIC	<i>sa685*</i>
<i>tax-4</i> IIIIC	<i>sa713*, sa731*, (sa697 = sa731)</i>
<i>unc-31</i> IVC	<i>sa534, sa681, sa684</i>
<i>unc-3</i> XR	<i>sa650, M3ff^a</i>
<i>pdk-1</i> XL	<i>sa680, sa709*, (sa652 = sa709)</i>
<i>akt-1</i> VC	<i>sa573, sa700</i>
<i>cam-1</i> IIC	<i>sa692</i>
<i>aex-6</i> IR	<i>sa699</i>
<i>hid-1</i> XL	<i>sa691, sa722</i>
<i>hid-2</i> XR	<i>sa698</i>
<i>hid-3</i> IC	<i>sa646</i>
<i>hid-4</i> IVC	<i>sa666</i>
<i>hid-5</i> XR	<i>sa725, (sa687 = sa725)</i>
<i>hid-6</i> I	<i>sa711</i>
<i>hid-7</i> IVC	<i>sa572</i>
Strong Dyf mutants	<i>sa551, sa554, sa555, sa660, sa682</i>
Possible weak Dyf mutants	<i>sa648, sa655, sa656, sa668, sa673, sa676, sa679, sa706, sa720</i>

Weak alleles of genes with strong Daf-c alleles at 25° are marked with an asterisk.

^a This *unc-3* mutant was lost before being given an allele number.

we might have expected to isolate more Dyf mutants. However, Dyf mutant dauers recover very poorly at 15° and have a greater tendency to climb up the sides of the plate and desiccate, so our screen probably was biased against their recovery. Nine other mutants (*sa648, sa655, sa656, sa668, sa673, sa676, sa679, sa706, sa720*) had weaker fluorescence and/or fewer cells dye filling and may carry weaker alleles of Dyf genes. Two of these (*sa673* and *sa676*) had dye-filling patterns consistent with defects specific to the ASI neuron, as has been reported for other Hid mutants such as *unc-3* and *cam-1* (PRASAD *et al.* 1998; KOGA *et al.* 1999). Weak Dyf mutants have been isolated before as strong suppressors of *daf-11* mutants (SCHACKWITZ 1996), suggesting that the dauer phenotypes of these genes are more sensitive than the Dyf phenotype to reduced levels of gene function. All of the mutants with putative dye-filling defects were kept but not subjected to further analysis.

A third type of expected mutation was *daf-3*. *daf-3* mutants are Hid and dye fill normally, but are Daf-d and do not respond to pheromone at 25° (AILION and THOMAS 2000). We used this combination of phenotypes to determine whether we had isolated any good

candidate *daf-3* mutations. Two mutants (*sa646* and *sa731*) exhibited no response to pheromone and had normal dye filling. As discussed in detail below, *sa731* is a new allele of *tax-4* and *sa646* defines a new gene on chromosome I. Thus, we may not have isolated any alleles of *daf-3* in our screen.

Mutants that were not strongly Daf-c at 25° and did not exhibit Dyf or Daf-d phenotypes were the best candidates for identifying new dauer genes. However, we could also isolate weak alleles of previously known Daf-c genes. Several of the strongest Hid mutants had a weak Daf-c phenotype at 25° and were candidates for such weak alleles. By mapping and complementation testing these mutants, we found that many were indeed weak alleles of known Daf-c genes. Some other strong Hid mutants that were not detectably Daf-c at 25° also proved to be weak alleles of known Daf-c genes. In all, we found 14 mutations that are weak alleles of known Daf-c genes: seven *daf-2*, one *daf-7*, three *daf-8*, two *tax-4*, and one *age-1* (Table 1). The large number of weak *daf-2* alleles is particularly striking given the fact that we isolated only one strong allele of *daf-2*.

Our quest for new dauer genes focused on mutants not assigned to any of the classes described above. We began by concentrating on mutants with the strongest Hid phenotypes. Several of these had Unc phenotypes that resembled *unc-31* or *unc-3*. By mapping and complementation testing, we demonstrated that we had indeed isolated three alleles of *unc-31* and two alleles of *unc-3* (Table 1). Thus, the screen was capable of identifying mutations in the desired class of genes. The following sections describe our characterization of other mutants isolated in the screen. Table 1 provides a summary of the best-characterized mutants and Table 2 summarizes map data. Figure 1 shows the map positions of the genes.

Characterization of Hid mutants: Our basic strategy for characterization of the Hid mutants began with observation of pleiotropic phenotypes, mapping the mutation to a chromosome, and complementation testing with known Daf-c mutants on that chromosome to identify weak Daf-c alleles (see above). For mutants of interest, double mutants were built with *daf-5* (which suppresses group II Daf-c mutants) and *daf-16* (which suppresses insulin branch Daf-c mutants) to get preliminary information about the position of the gene in the dauer pathway. Finally, we performed finer mapping with physically mapped markers to aid in the molecular identification of each gene of interest. The level of analysis varies from mutant to mutant. Generally, mutants with a stronger phenotype were analyzed in more detail, both for the scientific reason that their stronger phenotype suggests a greater role in dauer regulation and for the technical reason that their stronger phenotype made them easier to work with. Mutants that proved difficult to map, due to a weaker Hid phenotype or rapid dauer recovery, were set aside. All the mutations

TABLE 2
Map data

Mutation	Parental genotype	Animals picked	Result	Comment
<i>akt-1(sa573)</i> V	<i>akt-1/dpy-11</i>	Hid (<i>akt-1/akt-1</i>)	0/9 segregate Dpy	<i>akt-1</i> is linked to <i>dpy-11</i>
	<i>akt-1/dpy-11 unc-76</i>	Dpy non-Unc	<i>dpy-11</i> (4) <i>akt-1</i> (10) <i>unc-76</i>	<i>akt-1</i> is between <i>dpy-11</i> and <i>unc-76</i>
	<i>akt-1/dpy-11 rol-3</i>	Rol non-Dpy	<i>dpy-11</i> (8) <i>akt-1</i> (0) <i>rol-3</i>	<i>akt-1</i> is to the right of or close to <i>rol-3</i>
	<i>akt-1/rol-3 unc-42</i>	Rol non-Unc Unc non-Rol	<i>rol-3</i> (8) <i>akt-1</i> (0) <i>unc-42</i> <i>rol-3</i> (10) <i>akt-1</i> (0) <i>unc-42</i>	<i>akt-1</i> is to the right of or close to <i>unc-42</i>
	<i>akt-1/unc-42 sma-1</i>	Unc non-Sma Sma non-Unc	<i>unc-42</i> (2) <i>akt-1</i> (8) <i>sma-1</i> <i>unc-42</i> (2) <i>akt-1</i> (3) <i>sma-1</i>	<i>akt-1</i> is between <i>unc-42</i> and <i>sma-1</i>
	<i>akt-1/mDf1</i>		<i>mDf1</i> fails to complement <i>akt-1</i>	<i>akt-1</i> lies inside the region deleted by <i>mDf1</i>
	<i>egl-9/mDf1</i>	Wild type	<i>mDf1</i> complements <i>egl-9</i>	<i>akt-1</i> is left of <i>egl-9</i>
	<i>unc-42 akt-1/deg-3</i>	Egl non-Unc	<i>unc-42</i> (11) <i>akt-1</i> (23) <i>deg-3</i>	<i>akt-1</i> is between <i>unc-42</i> and <i>deg-3</i>
	<i>akt-1/unc-42 egl-9</i>	Hid (<i>cam-1/cam-1</i>)	<i>unc-42</i> (3) <i>akt-1</i> (4) <i>egl-9</i>	<i>akt-1</i> is between <i>unc-42</i> and <i>egl-9</i>
	<i>cam-1/dpy-10</i>	Dpy non-Unc	1/19 segregate Dpy	<i>cam-1</i> is linked to <i>dpy-10</i>
<i>cam-1(sa692)</i> II	<i>cam-1/dpy-10 unc-4</i>	Rol non-Unc	<i>dpy-10</i> (4) <i>cam-1</i> (3) <i>unc-4</i>	<i>cam-1</i> is between <i>dpy-10</i> and <i>unc-4</i>
	<i>cam-1/unc-4 bli-1 rol-1</i>	Rol non-Unc Bli non-Rol	<i>unc-4</i> (0) <i>cam-1</i> (7) <i>rol-1 bli-1</i> (0) <i>cam-1</i> (4) <i>rol-1</i>	<i>cam-1</i> is to the left of or close to <i>unc-4</i>
	<i>cam-1/rol-6</i>	Hid	0/16 segregate Rol	<i>cam-1</i> (ks52) Hid is linked to <i>rol-6</i>
<i>cam-1(ks52)</i> II	<i>aex-6/unc-101</i>	Con (<i>aex-6/aex-6</i>)	3/27 segregate Unc	<i>aex-6</i> is linked to <i>unc-101</i>
	<i>aex-6/eDf3</i>		<i>eDf3</i> complements <i>aex-6</i>	<i>aex-6</i> lies outside the region deleted by <i>eDf3</i>
<i>hid-1(sa691)</i> X	<i>unc-101 unc-59/eDf3</i>		<i>eDf3</i> complements <i>unc-101</i> but fails to complement <i>unc-59</i>	<i>aex-6</i> is to the left of <i>unc-59</i>
	<i>aex-6/unc-101 unc-59</i>	Unc-101 non-Unc-59	<i>unc-101</i> (86) <i>aex-6</i> (2) <i>unc-59</i>	<i>aex-6</i> is between <i>unc-101</i> and <i>unc-59</i> , much closer to <i>unc-59</i>
	<i>hid-1/lon-2</i>	Lon Hid	<i>unc-101</i> (7) <i>aex-6</i> (0) <i>unc-59</i> 1/8 segregate Hid 5/47 segregate Lon	<i>hid-1</i> is linked to <i>lon-2</i>
	<i>hid-1/lon-2 dpy-6</i>	Lon non-Dpy	<i>lon-2</i> (0) <i>hid-1</i> (11) <i>dpy-6</i>	<i>hid-1</i> is to the left of or close to <i>lon-2</i>
	<i>hid-1/unc-20 lon-2</i>	Lon non-Unc	<i>unc-20</i> (0) <i>hid-1</i> (17) <i>lon-2</i>	<i>hid-1</i> is to the left of or close to <i>unc-20</i>
	<i>hid-1/unc-1 dpy-3</i>	Dpy non-Unc Unc non-Dpy	<i>unc-1</i> (9) <i>hid-1</i> (0) <i>dpy-3</i> <i>unc-1</i> (3) <i>hid-1</i> (0) <i>dpy-3</i>	<i>hid-1</i> is to the right of or close to <i>dpy-3</i>
	<i>hid-1/dpy-3 unc-2</i>	Dpy non-Unc Unc non-Dpy	<i>dpy-3</i> (4) <i>hid-1</i> (4) <i>unc-2</i> <i>dpy-3</i> (1) <i>hid-1</i> (2) <i>unc-2</i>	<i>hid-1</i> is between <i>dpy-3</i> and <i>unc-2</i>
	<i>hid-1/dpy-3 lin-32 unc-2</i>	Unc non-Dpy	<i>dpy-3</i> (8) <i>lin-32</i> (27) <i>hid-1</i> (25) <i>unc-2</i> <i>yDf17</i> fails to complement <i>hid-1</i>	<i>hid-1</i> is between <i>lin-32</i> and <i>unc-2</i> <i>hid-1</i> lies inside the region deleted by <i>yDf17</i>
	<i>hid-1/yDf17</i>			
	<i>hid-2/lon-2</i>	Hid	15/40 segregate Lon	<i>hid-2</i> is linked to <i>lon-2</i>
<i>hid-2(sa698)</i> X	<i>hid-2/lon-2 dpy-6</i>	Lon non-Dpy	<i>lon-2</i> (8) <i>hid-2</i> (0) <i>dpy-6</i>	<i>hid-2</i> is to the right of or close to <i>dpy-6</i>
	<i>hid-2/dpy-6 unc-9</i>	Hid	1/17 segregate Dpy	<i>hid-2</i> is to the right of <i>dpy-6</i>
	<i>hid-2/dpy-6 unc-9</i>	Dpy non-Unc Unc non-Dpy	<i>dpy-6</i> (5) <i>hid-2</i> (3) <i>unc-9</i> <i>dpy-6</i> (2) <i>hid-2</i> (6) <i>unc-9</i>	<i>hid-2</i> is between <i>dpy-6</i> and <i>unc-9</i>

(continued)

TABLE 2
(Continued)

Mutation	Parental genotype	Animals picked	Result	Comment
<i>hid-3(sa646) I</i>	<i>hid-3/dpy-5</i>	Hid	4/22 segregate Dpy	<i>hid-3</i> is linked to <i>dpy-5</i>
	<i>hid-3/dpy-5 unc-75</i>	Dpy non-Unc Unc non-Dpy	<i>dpy-5</i> (1) <i>hid-3</i> (6) <i>unc-75</i> <i>dpy-5</i> (0) <i>hid-3</i> (7) <i>unc-75</i>	<i>hid-3</i> is between <i>dpy-5</i> and <i>unc-75</i>
	<i>hid-3/dpy-5 unc-29</i>	Dpy non-Unc Unc non-Dpy	<i>dpy-5</i> (1) <i>hid-3</i> (5) <i>unc-29</i> <i>dpy-5</i> (4) <i>hid-3</i> (0) <i>unc-29</i>	<i>hid-3</i> is between <i>dpy-5</i> and <i>unc-29</i>
	<i>hid-3/dpy-5 unc-13</i>	Dpy non-Unc Unc non-Dpy	<i>dpy-5</i> (8) <i>hid-3</i> (1) <i>unc-13</i> * <i>dpy-5</i> (11) <i>hid-3</i> (0) <i>unc-13</i>	<i>hid-3</i> is to the right of or close to <i>unc-13</i>
	<i>hid-3/dpy-14 unc-13</i>	Dpy non-Unc Unc non-Dpy	<i>dpy-14</i> (3) <i>hid-3</i> (0) <i>unc-13</i> <i>dpy-14</i> (15) <i>hid-3</i> (0) <i>unc-13</i>	<i>hid-3</i> is to the right of or close to <i>unc-13</i>
	<i>hid-3/unc-13 lin-10</i> <i>hid-3/sDf6</i>	Lin non-Unc	<i>unc-13</i> (3) <i>hid-3</i> (3) <i>lin-10</i> * <i>hid-3</i> complements <i>sDf6</i>	<i>hid-3</i> lies outside the region deleted by <i>sDf6</i>
<i>hid-4(sa666) IV</i>	<i>hid-4/unc-24 dpy-20</i>	Hid	0/25 segregate Unc or Dpy	<i>hid-4</i> is linked to <i>unc-24</i> and <i>dpy-20</i>
	<i>hid-4/unc-24 dpy-20</i> <i>hid-4/unc-24 daf-14</i>	Unc non-Dpy Unc non-Daf	<i>unc-24</i> (5) <i>hid-4</i> (9) <i>dpy-20</i> <i>unc-24</i> (11) <i>hid-4</i> (0) <i>daf-14</i>	<i>hid-4</i> is between <i>unc-24</i> and <i>dpy-20</i> <i>hid-4</i> is to the right of or close to <i>daf-14</i>
<i>hid-5(sa725) X</i>	<i>hid-5/unc-7</i>	Hid	4/27 segregate Unc	<i>hid-5</i> is linked to <i>unc-7</i>
	<i>hid-5/dpy-6 unc-9</i>	Dpy non-Unc Unc non-Dpy	<i>dpy-6</i> (8) <i>hid-5</i> (0) <i>unc-9</i> <i>dpy-6</i> (8) <i>hid-5</i> (0) <i>unc-9</i>	<i>hid-5</i> is to the right of or close to <i>unc-9</i>
<i>hid-6(sa711) I</i>	<i>hid-6/dpy-5</i>	Hid	0/12 segregate Dpy	<i>hid-6</i> is linked to <i>dpy-5</i>
	<i>hid-6/dpy-5 unc-29</i>	Dpy non-Unc Unc non-Dpy	<i>dpy-5</i> (0) <i>hid-6</i> (8) <i>unc-29</i> <i>dpy-5</i> (0) <i>hid-6</i> (8) <i>unc-29</i>	<i>hid-6</i> is to the left of or close to <i>dpy-5</i>
<i>hid-7(sa572) IV</i>	<i>hid-7/unc-5</i>	Hid	2/12 segregate Unc	<i>hid-7</i> is linked to <i>unc-5</i>
	<i>hid-7/unc-24 dpy-20</i>	Hid	2/10 segregate Dpy	<i>hid-7</i> is to the left of <i>dpy-20</i>
	<i>hid-7/unc-24 dpy-20</i>	Unc non-Dpy Dpy non-Unc	<i>unc-24</i> (5) <i>hid-7</i> (4) <i>dpy-20</i> <i>unc-24</i> (3) <i>hid-7</i> (5) <i>dpy-20</i>	<i>hid-7</i> is between <i>unc-24</i> and <i>dpy-20</i>

The results present map data in standard *C. elegans* nomenclature. The number of recombinants in each interval is given in parentheses. Results marked with an asterisk were anomalous (see MATERIALS AND METHODS).

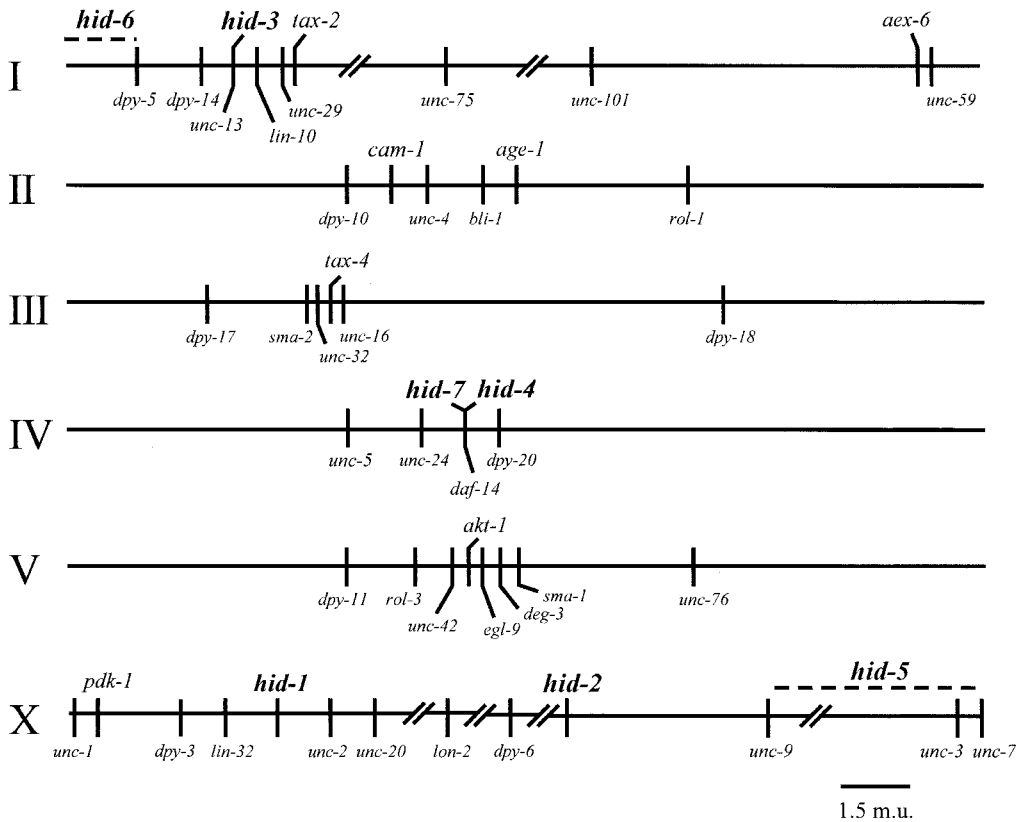


FIGURE 1.—Chromosomal positions of Hid mutants. Positions are shown relative to markers used in mapping.

studied in detail were recessive, as expected for loss-of-function mutations.

Catalog of Hid mutants: *unc-64*, *unc-31*, *unc-3*, and *egl-4*: Mutations in these four genes have been shown previously to have strong Hid phenotypes (AILION *et al.* 1999; DANIELS *et al.* 2000; AILION and THOMAS 2000). *unc-64* and *unc-31* encode proteins that regulate secretion and synaptic transmission (LIVINGSTONE 1991; ANN *et al.* 1997; OGAWA *et al.* 1998; SAIFEE *et al.* 1998). *unc-64* and *unc-31* mutants are not suppressed by *daf-5*, but are completely suppressed by *daf-16*, suggesting that they act in the insulin branch of the dauer pathway (AILION *et al.* 1999; AILION and THOMAS 2000). *unc-3* encodes a transcription factor (PRASAD *et al.* 1998) and *egl-4* has not been molecularly identified (HIROSE *et al.* 2003). *unc-3* and *egl-4* mutants are suppressed by *daf-5* and probably act in the group II branch of the dauer pathway (AILION and THOMAS 2000; DANIELS *et al.* 2000). We isolated three new alleles of *unc-31* and two new alleles of *unc-3* (Table 1), but did not isolate any alleles of *unc-64* or *egl-4*. Null alleles of *unc-64* are lethal (SAIFEE *et al.* 1998) and most *egl-4* mutant alleles have a relatively weak Hid phenotype (DANIELS *et al.* 2000), perhaps explaining our failure to isolate mutations in these genes.

tax-4(sa713, sa731) and *tax-2(sa1205)*: *tax-4* and *tax-2* encode subunits of a cyclic nucleotide-gated ion channel that appears to be part of the signal transduction machinery in the amphid sensory neuron endings (COBURN and BARG-

MANN 1996; KOMATSU *et al.* 1996). The *tax-4* and *tax-2* genes have both positive and negative effects on dauer formation, resulting in complex mutant phenotypes (COBURN *et al.* 1998; AILION and THOMAS 2000). The genes appear to function in the group I branch of the dauer pathway and probably elsewhere as well. We isolated two new alleles of *tax-4*. The Hid phenotype of *sa731* was not suppressed by mutations in *daf-5* and only weakly suppressed by mutations in *daf-16* (Table 3), consistent with function of *tax-4* in parallel to both the group II and the insulin branches of the dauer pathway.

We found *tax-2(sa1205)* in the background of an *unc-24* mutant strain. *tax-2(sa1205)* has a stronger Hid phenotype than other *tax-2* alleles and also has a weak Daf-c phenotype at 25°. We mapped *sa1205* close to the right of *unc-29* and showed that it failed to complement *tax-2(p691)* and *tax-2(ot25)* for the Hid phenotype, demonstrating that *sa1205* is a new allele of *tax-2*.

pdk-1(sa680, sa709): *sa680* mutants have a strong Daf-c phenotype at 25° and *sa709* is Daf-c only at 27°. These mutations define a new gene in the insulin branch of the pathway, *pdk-1*, which encodes a protein kinase that acts downstream of *age-1*. We presented a detailed analysis of these mutations elsewhere (PARADIS *et al.* 1999).

akt-1(sa573, sa700): These mutants are strongly Daf-c at 27°, but not at 25°. The only obvious pleiotropy is a tendency to stay near the border of the bacterial lawn (Bor phenotype) rather than dispersing. *sa573* was mapped to the chromosome V cluster and shown to

TABLE 3

Dauer formation in *daf-5* and *daf-16* double mutants with Hid genes at 27°

Genotype	% dauer formation at 26.8° (N)
N2	13 (201)
<i>daf-5(e1385)</i>	11 (110)
<i>daf-16(m27)</i>	4 (253) ^a
<i>akt-1(sa573)</i>	100 (148)
<i>akt-1(sa573); daf-5(e1385)</i>	94 (208)
<i>akt-1(sa573); daf-16(m27)</i>	10 (210) ^a
<i>aex-6(sa699)</i>	66 (165)
<i>aex-6(sa699); daf-5(e1385)</i>	26 (134)
<i>aex-6(sa699); daf-16(m27)</i>	1 (166) ^a
<i>hid-1(sa691)</i>	99 (186)
<i>hid-1(sa691); daf-5(e1385)</i>	79 (193)
<i>hid-1(sa691); daf-16(m27)</i>	18 (154) ^a
<i>hid-4(sa666)</i>	77 (182)
<i>hid-4(sa666); daf-16(m27)</i>	26 (208) ^a

Genotype	% dauer formation at 26.9° (N)
N2	13 (500)
<i>daf-5(e1385)</i>	10 (424)
<i>daf-16(m27)</i>	11 (472) ^a
<i>hid-1(sa1058)</i>	99 (313)
<i>hid-1(sa1058); daf-5(e1385)</i>	89 (357)
<i>hid-1(sa1058); daf-16(m27)</i>	14 (416) ^a
<i>hid-2(sa698)</i>	92 (374)
<i>hid-2(sa698); daf-5(e1385)</i>	78 (411)
<i>hid-2(sa698); daf-16(m27)</i>	12 (416) ^a

Genotype	% dauer formation at 27.0° (N)
N2	11 (246)
<i>daf-5(e1385)</i>	3 (231)
<i>daf-16(m27)</i>	2 (199)
<i>cam-1(sa692)</i>	98 (164)
<i>cam-1(sa692); daf-5(e1385)</i>	70 (92)
<i>cam-1(sa692); daf-16(m27)</i>	ND ^b
<i>tax-4(sa731)</i>	100 (173)
<i>tax-4(sa731); daf-5(e1385)</i>	99 (143)
<i>tax-4(sa731); daf-16(m27)</i>	84 (239) ^a

The number in parentheses is the number of animals counted. Each section of the table consists of counts performed at the same time on the same shelf of an incubator.

^a Partial dauers as described (VOWELS and THOMAS 1992).

^b ND, not determined. Almost all the animals failed to hatch or died as L1. Of the very few animals that did not die at an early stage, some formed partial dauers and some did not, suggesting that there might be partial suppression by *daf-16*, but with so few animals it is difficult to interpret.

complement *daf-11*, the only known Daf-c gene in this region. The Hid phenotype of *sa573* was strongly suppressed by mutations in *daf-16* but only weakly suppressed by mutations in *daf-5* (Table 3), suggesting that the gene functions in the insulin branch of the dauer pathway.

To facilitate molecular characterization, we mapped *sa573* to a narrow region of chromosome V between *unc-42* and *egl-9* (Table 2; Figure 1). A good candidate gene in this region was *akt-1*, which encodes a protein kinase downstream of *age-1* in the insulin branch of the dauer pathway. The *akt-1(mg144gf)* gain-of-function mutation suppresses the Daf-c phenotype of *age-1* mutants in the insulin branch (PARADIS and RUVKUN 1998), but no loss-of-function mutations in *akt-1* have been described. Inhibition of *akt-1* activity by dsRNA interference (RNAi) did not lead to a Daf-c phenotype at 25°; however, RNAi of both *akt-1* and *akt-2* (a second worm Akt homolog) resulted in a Daf-c phenotype at 25°, suggesting that *akt-1* and *akt-2* are at least partially redundant (PARADIS and RUVKUN 1998). *mgEx338*, an extrachromosomal array carrying functional *akt-1* (PARADIS and RUVKUN 1998), significantly suppressed the Hid phenotype of *sa573*, suggesting that *sa573* is an *akt-1* allele. To confirm this, we sequenced *akt-1(sa573)* and found a single G202R missense mutation at a conserved residue near the amino terminus of the kinase domain. Subsequent phenotypic and complementation analysis showed that *sa700*, another mutation from our screen, also affects *akt-1* and results in a G205E missense mutation, only three amino acids away from the *sa573* mutation. Thus, *sa573* and *sa700* are the first identified loss-of-function mutations in the *akt-1* gene. Since *akt-1* mutants have a 27° Daf-c phenotype on their own, the *akt-1* gene cannot be completely redundant with *akt-2*. No loss-of-function or gain-of-function mutations have yet been isolated in *akt-2*.

cam-1(sa692, ks52): We isolated the *sa692* mutant, which is strongly Daf-c at 27° and weakly Daf-c at 25°. In addition to the Hid phenotype, *sa692* mutants have several pleiotropic phenotypes, including a distinctive Unc phenotype, characterized by movement with a higher amplitude waveform and frequent direction reversals. *sa692* mutants also are frequently thinner in the posterior part of the body, a phenotype referred to as withered tail (Wit; FORRESTER *et al.* 1998), and are occasionally Egl. Filling the amphid neurons of *sa692* animals with the fluorescent dye FITC revealed abnormalities in cell position: the ASK, ADL, and ASI neurons were sometimes separated from one another and frequently were located posterior to the posterior bulb of the pharynx. The Hid phenotype of *sa692* was partially suppressed by *daf-5*, but suppression by *daf-16* could not be analyzed due to a high rate of lethality in the *daf-16; sa692* double mutant at 27° (Table 3).

We mapped *sa692* to the center of chromosome II (Table 2; Figure 1). *cam-1* (also known as *kin-8*) maps to this region and encodes a receptor tyrosine kinase of the ROR family (KOGA *et al.* 1999). The *cam-1(ks52)* mutation is a deletion of the entire kinase domain and was reported to have a weak Daf-c phenotype on old lawns of *Escherichia coli* (KOGA *et al.* 1999). On plates with our normal *E. coli* lawns, we found that *cam-1(ks52)*

TABLE 4
Pleiotropic phenotypes of *hid-1* mutants

Genotype ^a	% dauers at 26.9° (N)	Unc	Con	% EMC ^b	Defecation cycle time ^c
N2	6 (216)	+	+	90 (60)	45.3 ± 2.7
<i>hid-1(sa691)</i>	93 (238)	–	–	23 (60)	38.5 ± 5.4
<i>hid-1(sa691)/yDf17</i>	ND ^d	–	–	ND	ND
<i>hid-1(sa1056)</i>	75 (316)	–	–	30 (60)	39.4 ± 3.1
<i>hid-1(sa1058)</i>	99 (234)	–	–	23 (60)	39.9 ± 4.0
<i>hid-1(sa722)</i>	ND	–	–	ND	ND

ND, not determined.

^a The complete genotype is given except in the case of *hid-1(sa691)/yDf17* where the complete genotype is *mnDp66/+; him-8(e1489)/+; hid-1(sa691) lon-2(e678)/yDf17*.

^b The percentage of defecation motor programs (DMPs) that had an enteric muscle contraction (EMC), with the number of DMPs in parentheses. Ten DMPs were observed per animal. One N2 animal missed five EMCs, which is atypical.

^c Mean cycle time (interval between successive DMPs) in seconds ±SD.

^d Animals heterozygous for *yDf17* were extremely slow growing at 27° and could not be reliably scored for a dauer phenotype.

made 35% dauers at 25.6° and 99% dauers at 26.8°. In 24 hr, 98% of the dauers recovered at 25.6°, while only 5% of the dauers recovered at 26.8°. We showed that the Hid phenotype of *cam-1(ks52)* maps near *sa692* and that some *cam-1(ks52)* animals are Unc and Wit, similar to the *sa692* mutant. *sa692* and *cam-1(ks52)* failed to complement for the Hid phenotype, and all *sa692* phenotypes were rescued by a *cam-1(+)* genomic clone in 4/4 transgenic lines. We conclude that *sa692* is a new allele of *cam-1*.

Why does *sa692* have more severe phenotypes than the *ks52* deletion allele does? A likely possibility is that *ks52* is not a null mutation, since it retains the putative extracellular and transmembrane domains of the receptor. *cam-1* was independently identified from a screen for defects in CAN cell migration, which can cause the withered tail phenotype (FORRESTER *et al.* 1998, 1999). Several of these mutants have early stop codons in *cam-1* and more severe phenotypes than *ks52* does (FORRESTER *et al.* 1998, 1999). Thus, the *sa692* phenotype is more similar to that of putative null alleles, and *ks52* probably retains some gene activity. If so, the function of *cam-1* in regulating dauer formation appears to depend on the kinase domain, while the function of *cam-1* in regulating movement and cell migration does not.

aex-6(sa699): *sa699* mutant animals are Daf-c at 27°, but not at 25°. The Daf-c phenotype at 27° is weaker than that of the Hid mutants discussed previously (Table 3), but a strong defect in dauer recovery at 27° facilitated analysis. In addition to the Hid phenotype, *sa699* mutants have a strong constipated (Con) phenotype, are somewhat lethargic and Egl, and are moderately resistant to the acetylcholinesterase inhibitor aldicarb (data not shown). Initial mapping placed *sa699* on the right arm of chromosome I. Mutations in two genes (*aex-5* and *aex-6*) cause Con phenotypes and map to this region

(THOMAS 1990). Analysis of the previously isolated *aex-6(sa24)* mutant showed that it has a Hid phenotype, although weaker than that of *sa699*. Furthermore, *sa699* complemented *aex-5(sa23)* for the Con phenotype but failed to complement *aex-6(sa24)* for both the Hid and Con phenotypes, indicating that *sa699* is a new allele of *aex-6*. *sa24* shares the lethargic and Egl phenotypes of *sa699*, indicating that these pleiotropies are all from mutations in a single gene. The Hid phenotype of *sa699* was strongly suppressed by mutations in *daf-16* but only partially suppressed by mutations in *daf-5* (Table 3), suggesting that the gene functions in the insulin branch of the dauer pathway. We refined the map position of *aex-6* to close to the left of *unc-59* (Table 2; Figure 1).

hid-1(sa691, sa722, sa1056, sa1058): The *sa691* and *sa722* mutations were isolated in our screen and cause a strong Daf-c phenotype at 27°, but not at 25°. They share several other pleiotropic phenotypes (Table 4). *sa691* animals have lethargic, mildly uncoordinated movement and do not move well in response to touch (Unc phenotype). *sa691* mutants also have a moderate Con phenotype that results from defective aBoc and Exp steps of the defecation motor program (DMP), called the Aex phenotype (THOMAS 1990). We quantified the defecation defect by determining the percentage of DMPs with a normal Exp step (Table 4, % EMC). The *sa691* mutant has ~20% EMC. Furthermore, the defecation cycle period of *sa691* animals was shorter than that of wild type (Table 4), a phenotype referred to as Dec-s (IWASAKI *et al.* 1995).

We initially mapped *sa691* to the left arm of the X chromosome (Table 2). Two Aex genes, *aex-3* and *aex-4*, map in this region. We showed that *sa691* complements both *aex-3(ad418)* and *aex-4(sa22)* for all of its phenotypes, indicating that it is not allelic to either of these genes. The Hid phenotype of *sa691* was strongly sup-

TABLE 5
Interactions of *hid-3* with *daf-c* genes

Genotype	% dauer formation at 25.4° (N)	% dauer formation at 15° (N)
<i>daf-11(sa195)</i>	100 (464)	36 (464)
<i>hid-3(sa646); daf-11(sa195)</i>	44 (473)	39 (551)
<i>daf-7(e1372)</i>	100 (377)	63 (403)
<i>hid-3(sa646); daf-7(e1372)</i>	100 (523)	66 (529)
<i>daf-2(e1370)</i>	100 (571)	ND
<i>hid-3(sa646); daf-2(e1370)</i>	100 (438)	ND

Each count shows the total of two plates counted at the same time. The number in parentheses is the number of animals counted. ND, not determined.

pressed by mutations in *daf-16* but only weakly suppressed by mutations in *daf-5* (Table 3), suggesting that the gene functions in the insulin branch of the dauer pathway.

To facilitate molecular characterization, we mapped *sa691* to a narrow region of the X chromosome between *lin-32* and *unc-2* (Table 2; Figure 1). The Unc, Con, and Hid phenotypes were not separated in any recombinants, indicating that they are tightly linked. No previously described mutants with Unc, Con, or Daf-c phenotypes map to this interval, suggesting that *sa691* defines a new gene, which we named *hid-1*. To investigate the nature of the *sa691* allele, we examined the phenotype of *sa691* placed over *yDf17*, a deficiency that deletes *hid-1*. *sa691/Df* animals had Unc and Con phenotypes that resembled those of the *sa691* homozygote, consistent with *sa691* being a strong loss-of-function allele (Table 4). To isolate more alleles of *hid-1*, we performed a noncomplementation screen (see MATERIALS AND METHODS). We isolated two more alleles of *hid-1* (*sa1056*, *sa1058*), which had Hid, Unc, Con, and Dec-s phenotypes both qualitatively and quantitatively similar to those of *sa691* (Table 4 and data not shown). Thus, these phenotypes are all caused by mutation of *hid-1*. The pleiotropic phenotypes of *hid-1* mutants suggest that the gene regulates the function of neurons. Like *sa691*, *hid-1(sa1058)* was strongly suppressed by mutations in *daf-16* but only weakly suppressed by mutations in *daf-5* (Table 3).

hid-2(sa698): *hid-2(sa698)* is strongly Daf-c at 27° and very weakly Daf-c at 25°. It has no obvious pleiotropies. *hid-2* was strongly suppressed by *daf-16* and weakly suppressed by *daf-5* (Table 3), suggesting that the gene functions in the insulin branch of the dauer pathway. We mapped *hid-2* to the X chromosome between *dpy-6* and *unc-9*, a region with no known Daf-c genes. Hence, *sa698* probably defines a new gene.

hid-3(sa646): *hid-3(sa646)* is strongly Daf-c at 27°, but not at 25°. *hid-3(sa646)* formed no dauers in response to dauer-inducing pheromone at ≤25°. The Hid and pheromone-insensitive phenotypes appear to be tightly linked, but it is not yet clear whether they are both

due to mutation of the same gene (see MATERIALS AND METHODS). The combination of Hid and pheromone-insensitive phenotypes is also seen in *daf-3*, *tax-2*, and *dyf* mutants (AILION and THOMAS 2000). However, *hid-3* shows normal dye filling with FITC and DiI and maps to a location distinct from *daf-3* and *tax-2* (Table 2; Figure 1). *tax-2* suppresses the Daf-c phenotype of group I Daf-c mutants (e.g., *daf-11*), whereas *daf-3* suppresses group II Daf-c mutants (e.g., *daf-7*), and neither suppresses mutants in the insulin branch (e.g., *daf-2*; THOMAS *et al.* 1993; COBURN *et al.* 1998). To see whether *hid-3* had other similarities to *daf-3* or *tax-2*, we built double mutants of *hid-3* with *daf-11*, *daf-7*, and *daf-2*. As shown in Table 5, *hid-3* partially suppressed *daf-11* at 25°, but did not suppress *daf-7* or *daf-2*. This suggests that *hid-3* is most similar to *tax-2* and may function in the group I branch of the pathway. Consistent with this, the Hid phenotype of *hid-3* is not suppressed by mutations in *daf-5* (data not shown).

hid-4(sa666): *hid-4(sa666)* is strongly Daf-c at 27°, but not at 25°. *hid-4* dauers recover fairly well at 27°. *hid-4* was partially suppressed by *daf-16* (Table 3), suggesting that it acts at least partially in parallel to the insulin branch of the pathway. *hid-4* was mapped to chromosome IV close to the position of the group II Daf-c gene *daf-14* (Table 2; Figure 1). However, *hid-4(sa666)* lacks the dark intestine and Egl pleiotropies of *daf-14* mutants and it complements *daf-14* for the Daf-c phenotype at 27° and thus appears to define a new gene.

hid-5(sa725), *hid-6(sa711)*, and *hid-7(sa572)*: These three mutants are strongly Daf-c at 27°, but not at 25°. *hid-5(sa725)* appears to be weakly clumpy and Egl; *hid-6(sa711)* and *hid-7(sa572)* have no obvious pleiotropies. They were assigned new gene names because they map to regions with no known dauer genes. *hid-5* maps to the right arm of the X chromosome, probably to the right of *unc-9* (Table 2; Figure 1). *hid-5* complemented *hid-2*, which maps between *dpy-6* and *unc-9*. The only other Daf gene on this chromosome arm is *unc-3*, which has a distinctive uncoordinated coiler phenotype. *hid-5* has normal movement and thus is probably distinct from *unc-3*. *hid-6* maps to chromosome I, probably to the left

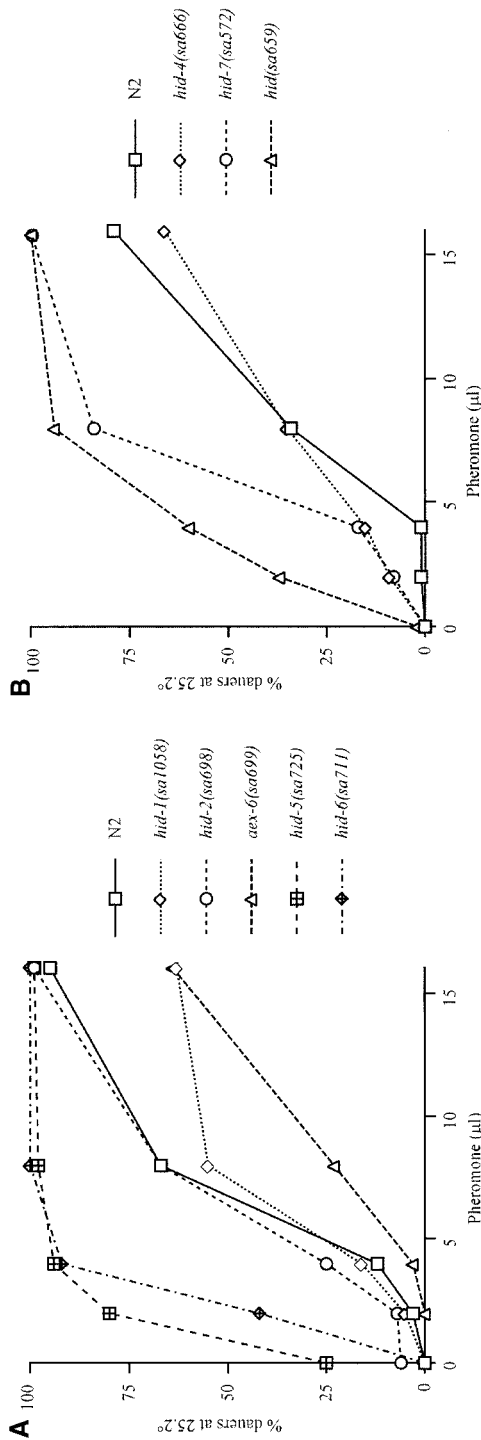


FIGURE 2.—Dauer formation of various Hid mutants in response to exogenous pheromone. Each graph plots the percentage of animals that formed dauers in response to different concentrations of pheromone at 25°. Approximately 100–200 animals were counted at each concentration of pheromone. All strains were outcrossed twice before the assay, except for *hid-7(sa572)*, which was not outcrossed. *hid(sa659)* was not mapped carefully or assigned a gene name.

of *dpy-5* (Table 2; Figure 1). *hid-6* complemented *daf-8*, which also map to chromosome I. *hid-7* maps to chromosome IV, between *unc-24* and *dpy-20*. *hid-7* complemented *daf-14* and *hid-4*, which also map to this interval. Epistasis of *hid-5*, *hid-6*, and *hid-7* with *Daf-d* mutations was not examined.

Pheromone sensitivity of Hid mutants: We previously showed that some Hid mutants (*e.g.*, *unc-64*, *unc-31*, *unc-3*, and *egl-4*) are hypersensitive to dauer pheromone at lower temperatures in addition to being *Daf-c* at 27° (AILION and THOMAS 2000; DANIELS *et al.* 2000). This result indicates that these mutants are generally sensitized to dauer induction, rather than being specifically sensitized to high temperatures. We measured the pheromone sensitivity of some of the new Hid mutants at 25° (Figure 2). *hid-5(sa725)*, *hid-6(sa711)*, *hid-7(sa572)*, and *hid(sa659)* are clearly hypersensitive to pheromone. *aex-6(sa699)*, *hid-1(sa1058)*, *hid-2(sa698)*, and *hid-4(sa666)* have pheromone responsiveness similar to or weaker than that of N2. Thus, pheromone hypersensitivity is a property of many Hid mutants, but not all.

Double mutants with *pdk-1(gf)* and *akt-1(gf)*: The *pdk-1(mg142gf)* and *akt-1(mg144gf)* dominant gain-of-function mutations were isolated as suppressors of *age-1*, but do not suppress *daf-2* (PARADIS and RUVKUN 1998; PARADIS *et al.* 1999). This suggests that there is a bifurcation of the insulin signaling pathway downstream of *daf-2*, with one subbranch consisting of *age-1*, *pdk-1*, and *akt-1*. We previously reported that *unc-64* and *unc-31* mutants are well suppressed by *daf-16*, but not suppressed by *pdk-1(mg142gf)* or *akt-1(mg144gf)* (AILION and THOMAS 2000). *hid-1* and *aex-6* are also strongly suppressed by *daf-16* (Table 3), suggesting that they function in the insulin branch of the dauer pathway. To examine whether they act in the *age-1* subbranch, we built double mutants with *pdk-1(mg142gf)* and *akt-1(mg144gf)*. Both *hid-1* and *aex-6* were partially suppressed by *akt-1(mg144gf)* and only weakly suppressed by *pdk-1(mg142gf)* (Table 6). This could indicate that these genes function in the *age-1* subbranch of the insulin pathway, but is also consistent with function in parallel to this branch. The stronger suppression by *akt-1(mg144gf)* may be because it activates the pathway more strongly than *pdk-1(mg142gf)* or may reflect additional nonlinear aspects of the pathway. *akt-1(sa573)* was not suppressed by *pdk-1(mg142gf)*, as expected if *pdk-1* acts directly upstream of *akt-1*.

A striking observation is that both *hid-1* and *aex-6* double mutants with *akt-1(mg144gf)* [and perhaps *pdk-1(mg142gf)*] formed some full dauers, some non-dauers, and some partial dauers that resembled *daf-16* partial dauers (VOWELS and THOMAS 1992). This is a surprising result for several reasons. First, *akt-1(mg144gf)* forms normal dauers on its own when starved or induced by pheromone (PARADIS and RUVKUN 1998) and forms normal dauers in double mutants with *pdk-1(sa680)* or group II *Daf-c* mutants (PARADIS *et al.* 1999; INOUE and

TABLE 6
Dauer formation in double mutants of *Hid* genes with *pdk-1(gf)*, *akt-1(gf)*, and *sa315*

Genotype	Phenotype at 26.9° (%)			N ^b
	L4 larvae and adult	Dauer	Partial dauer ^a	
N2	63	37	0	206
<i>akt-1(mg144gf)</i>	95	3	2	147
<i>pdk-1(mg142gf)</i>	25	75 ^c	0	236
<i>sa315</i>	100	0	0	224
<i>unc-64(e246)</i>	0	100	0	53
<i>unc-64(e246); akt-1(mg144gf)</i>	17	83 ^d	0	127
<i>unc-64(e246); pdk-1(mg142gf)</i>	0	100	0	186
<i>unc-64(e246); sa315</i>	100	0	0	232
<i>unc-31(e928)</i>	2	98	0	103
<i>unc-31(e928); akt-1(mg144gf)</i>	1	99	0	178
<i>unc-31(e928); pdk-1(mg142gf)</i>	0	100	0	75
<i>unc-31(e928); sa315</i>	99	0	1	97
<i>akt-1(sa573)</i>	0	100	0	135
<i>akt-1(sa573); pdk-1(mg142gf)</i>	0	100	0	203
<i>hid-1(sa691)</i>	1	99	0	109
<i>hid-1(sa691); akt-1(mg144gf)</i>	31	35	34	217
<i>hid-1(sa691) pdk-1(mg142gf)</i>	5	92	3	324
<i>hid-1(sa691); sa315</i>	100	0	0	371
<i>aex-6(sa699)</i>	40	60	0	131
<i>aex-6(sa699); akt-1(mg144gf)</i>	59	18	24	148
<i>aex-6(sa699); pdk-1(mg142gf)</i>	28	72	0	171
<i>aex-6(sa699); sa315</i>	100	0	0	151
N2	91	9	0	125
<i>aex-6(sa699)</i>	3	97	0	117
<i>aex-6(sa699); akt-1(mg144gf)</i>	74	0	26	88
<i>aex-6(sa699); pdk-1(mg142gf)</i>	39	61	0	228

The top part of the table shows the results from a single experiment and the bottom part shows the results of a few strains in a different experiment.

^a These were radially constricted animals that resembled dauers, but were lighter in appearance, moved more, and had occasional pumping. They had alae and hypodermal bodies, but did not have refractile material in the gut, and the pharynx appeared much closer to an L3 pharynx than to a dauer pharynx. This suggests they are very similar and perhaps identical to the partial dauers formed by *daf-16* (VOWELS and THOMAS 1992).

^b The number of animals scored.

^c This is an unusually high value for dauer formation in *pdk-1(mg142gf)* mutants.

^d In all other assays except this one, *akt-1(mg144gf)* showed no suppression of *unc-64*.

THOMAS 2000b). It does form abnormal dauer-like animals in double mutants with *daf-2* (PARADIS and RUVKUN 1998), but these are distinct from the partial dauers characteristic of *daf-16* mutants and the partial dauers seen here. Second, to our knowledge these are the first examples of strains capable of forming both normal and partial dauers; *daf-16* mutants always form partial dauers or non-dauers.

We also built double mutants with *sa315*, a *Daf-d* mutant with phenotypes similar to those of *daf-16* (e.g., formation of partial dauers) and a probable site of action in the insulin pathway (INOUE and THOMAS 2000b). Like *daf-16*, *sa315* completely suppressed *unc-64*, *unc-31*, *hid-1*, and *aex-6* (Table 6). This provides further support for assignment of these genes to the insulin branch of the dauer pathway.

Double mutants with Syn-Daf genes: To see whether the new *Hid* mutants were Syn-Daf, we built some double mutants between these genes and the previously characterized Syn-Daf genes *unc-64*, *unc-31*, *unc-3*, and *osm-6*. As shown in Table 7, a few of the combinations are weakly *Daf-c*, but none have the strong *Daf-c* phenotype characteristic of some Syn-Daf combinations.

Molecular analysis of *hid-1*: We cloned *hid-1* by transgenic rescue of the *Hid*, *Unc*, and *Con* phenotypes with cosmid clones and subclones (see MATERIALS AND METHODS). A subclone carrying only one predicted gene, K02E10.2, rescued all of the *hid-1* phenotypes, suggesting that K02E10.2 is the *hid-1* gene. This gene has 15 exons and is predicted to encode a protein of 729 amino acids (Figure 3, A and C). Sequencing of *hid-1* mutant alleles confirms the gene assignment. *sa691*

TABLE 7

Syn-Daf phenotypes of Hid mutants

Genotype	% dauer formation at 25° (N)
<i>unc-64(e246)</i>	19 (107)
<i>unc-31(e928)</i>	1 (153)
<i>unc-3(e151)</i>	2 (249)
<i>aex-6(sa699)</i>	0 (152)
<i>akt-1(sa573)</i>	0 (109)
<i>hid-1(sa691)</i>	0 (10)
<i>hid-4(sa666)</i>	0 (162)
<i>osm-6(p811)</i>	0 (85)
<i>unc-64(e246); akt-1(sa573)</i>	27 (181)
<i>unc-31(e928); akt-1(sa573)</i>	34 (175)
<i>akt-1(sa573); unc-3(e151)</i>	17 (175)
<i>aex-6(sa699); unc-31(e928)</i>	0 (89)
<i>aex-6(sa699); unc-3(e151)</i>	27 (123)
<i>aex-6(sa699); osm-6(p811)</i>	7 (46)
<i>osm-6(p811); hid-1(sa691)</i>	8 (62)
<i>hid-4(sa666); unc-3(e151)</i>	9 (236)
<i>aex-6(sa699); hid-1(sa1058)^a</i>	2 (108)

^a This strain was assayed in a separate experiment in which the *aex-6(sa699)* and *hid-1(sa1058)* single mutants formed no dauers.

mutates the exon 9 splice acceptor. *sa1056* has two separate mutations: a mutation in the exon 13 splice donor and a D718V missense mutation. *sa1058* has a G307E missense mutation. *sa722* has a stop codon at W112, and thus may be a null mutation. The *hid-1* gene encodes a novel protein that appears to have a single strongly conserved homolog in human, mouse, and *Drosophila melanogaster* (Figure 3C). No close relatives were found in BLAST searches of the *C. elegans* genome. A composite hydropathy plot of HID-1 proteins from *C. elegans*, *Drosophila*, and humans suggests that the proteins have many transmembrane domains (Figure 3B). No other obvious functional domains were found in the predicted protein sequence.

We constructed a *hid-1::gfp* fusion to examine expression of *hid-1*. Expression of GFP was observed in adults in some neurons in the head, tail, and nerve ring, but was too faint to permit identification of specific cells (data not shown). Consistent with this result, a *hid-1::lacZ* fusion construct, made as part of a large gene expression project, was expressed at all developmental stages in neurons of the head, tail, and ventral nerve cord (I. HOPE, personal communication; <http://www.wormbase.org/>). Occasional faint expression was also reported in the metacarpus and terminal bulb of the pharynx.

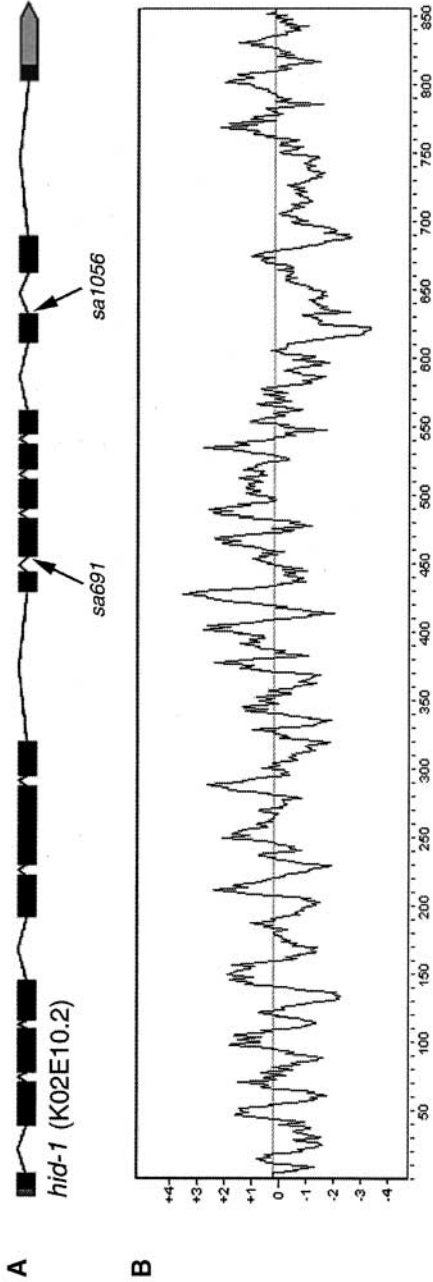
DISCUSSION

Here we present the results of a screen for Daf-c mutants at 27° and the characterization of some of the mutants. The hope was that this screen would be able to isolate mutations in new genes that cause a strong Daf-c phenotype at 27° but not at 25°, the temperature of previous screening attempts. New alleles of *unc-31* and *unc-3*, two previously known genes with these phenotypes, were recovered in the screen. Furthermore, we identified at least 10 genes that had not been identified before at 25°. Since we isolated only one allele of many genes, we clearly did not screen to saturation and there are assuredly more Hid mutants to be found.

For reasons that are not yet apparent, the 27° screen appears to be particularly sensitive to isolating mutants in the insulin branch of the dauer pathway. We isolated eight mutations in *daf-2* alone, seven of which were weak mutations that do not cause a Daf-c phenotype at 25°. The isolation of new genes in the insulin branch is useful since the only genes in this branch identified as Daf-c at 25° were *daf-2* and *age-1*, suggesting that other genes do not have such strong Daf-c phenotypes. Two of these genes were identified in our screen: the *pdh-1* and *akt-1* protein kinase genes, which function downstream of *age-1* in the signal transduction cascade. Our identification of Daf-c loss-of-function mutations in *pdh-1* and *akt-1* complements the identification of gain-of-function mutations in these genes as suppressors of *age-1* (PARADIS and RUVKUN 1998; PARADIS *et al.* 1999). The phosphorylated lipid second messengers produced by PI3K (encoded by the *age-1* gene in *C. elegans*) have been shown to bind many targets *in vitro* (TOKER and CANTLEY 1997), but the *in vivo* targets of this signaling cascade were not known. The PDK1 and Akt kinases had been identified biochemically as possible targets, and the identification of mutations in these genes here provides strong evidence that these are important *in vivo* targets of the PI3K signal transduction pathway.

In addition to the relatively well-defined branch of the insulin pathway that proceeds linearly from *daf-2* through *age-1*, *pdh-1*, and *akt-1*, there appears to be a less well-defined branch downstream of *daf-2* in parallel to the *age-1* branch. Existence of this branch is inferred from the lack of suppression of *daf-2* mutants by the *pdh-1* and *akt-1* gain-of-function mutations that completely suppress *age-1* (PARADIS and RUVKUN 1998; PARADIS *et al.* 1999). Some of our new genes may be acting in this second branch. Mosaic analysis of *daf-2* shows that it functions cell nonautonomously, and it has been proposed that signaling by DAF-2 leads to the produc-

FIGURE 3.—*hid-1* encodes a novel, conserved transmembrane protein. (A) *hid-1* gene structure as inferred from sequencing of cDNA yk32f11. (B) Composite hydropathy plot of the *C. elegans*, *D. melanogaster*, and human HID-1 proteins (made with Bonsai 1.1; <http://calliope.gs.washington.edu/software/>). (C) Alignment of the *C. elegans*, *D. melanogaster*, and human HID-1 proteins. Alignments were made with Bonsai 1.1 and presented graphically with Boxshade 3.21.



C

W->stop sa722

ceHID-1	1	MGAQGRVDFKQVLLDVRSP	---GKDETEFDQAMP	--DSVNEIFAMISGDIRKLRDESPKNIATLVYVEKLFQSRNHPATIDQKK--TI
dmHID-1	1	MGNTDSKLNFRKAVOL	TKNOKIDSDSQEWFQCHOTLEVALVTSERIQENENPANAATLCKNAVEKLAQAVDSSCRTQAEQQCVL	
hhID-1	1	MGSTDSELNFRKAVIQL	FTPTQVZATDDAFWDQFWADPATSVDVFAVLPAAEIRAVEREESPENLATLCHFAVEKLVQGAESGCHSEKKEKQIVL	
ceHID-1	89	MAIRLLETRIVPYLLEDAEMRGYFWSPI	-----HGDAAKPLAAVLEETLSDLLFCPEFTLTHAN---	GOKIDDLSTIDSCYEIWEAGVGS
dmHID-1	96	NCVRLVRCLEPYLFEDEKWRDFWBSLP	-----SQDKTMPLAOSLLNATCDLLFCPDTATRRACPEKAEELANI	DSCEYIWEAGVGF
hhID-1	96	NCSRLLETRVLPYLFEDPDWEGFWSYF	PGACRGCGQGEDEDEHARPEL	ESLLAIAADLLFCPDTVQSHRRRSYVDSAEDEVHSLDSCYEIWEAGVGF
ceHID-1	171	GKPPNVALHYQNRTEILKLLLTCEFAELIYAPVS	--DETRLRWVIRHETSVPHPVLPETSLLNIVCAYPDVGGLPYNVLLFNDRSREPLVELAL	
dmHID-1	181	AQSPPHNAHMERRTEILKLLLTCEFSPPMYRSPQ	-QSEPPNKWIAVFTSADNRHALPFTSFLNVTCSYDPVGFQVPMHLLPAPTEPLVACL	
hhID-1	191	AHSPPQNYIHDHNMELKLLLTCESEAMYLPAPESGCTNPMVQF	CSTENRHALPFTSLLNIVCAYPDVGGLPYNVLLFNDRSREPLVLEAAA	
ceHID-1	264	QVLVCGDKKETQPNNTDSC	-----YKDNFFINYLSHHREEDDFMLKGTIRLLSNLHSSSYLPNSKRVNFHQBLLVLLMVKC	
dmHID-1	275	QLLVLDHDMVYQQLTQFGQASVDEGNCG	-----DNEFINYLSSVHRDEDFVLRKGTIRLLSNLPLVQNV	-YLPNSKRLHCHQBLLVLLMVKI
hhID-1	286	QVLVLDHDSASASPVTVDGTTTCTAMDDADPPGPE	NEFINYLSSVHRDEDFVLRKGTIRLLSNLPLVQNV	-YLPNSKRLHCHQBLLVLLMVKI
ceHID-1	344	CEINQKPMFYVLRKTSVDLILVPILVHI	SDARNDSGRVGLIHMGVFI	ILLSGERNFGVRLNKPPTAKANINVQFTGSHADLLLVHKLITTTG
dmHID-1	363	CDYNKRELYFVLRKSDVLDLILVPILVH	LNYSRADQSRVGLMHI	GVFI
hhID-1	379	CDFNKRELYFVLRKSDVLDLILVPILVH	LNYSRADQSRVGLMHI	GVFI
ceHID-1	439	NYRLQFLDFCLTITMNVNVPYMKLSMVAANKD	VHLVEAFSTPWFPSPTNPQLVFSLELVFNVMIOYQFDGNSNLVYTI	IRKRNVFYQLSNLIS
dmHID-1	458	HQRLOPLDFCLTITMNVNVPYMKLSMVAANKD	VHLVEAFSTPWFPSPTNPQLVFSLELVFNVMIOYQFDGNSNLVYTI	IRKRNVFYQLSNLIS
hhID-1	474	HQRLOPLDFCLTITMNVNVPYMKLSMVAANKD	VHLVEAFSTPWFPSPTNPQLVFSLELVFNVMIOYQFDGNSNLVYTI	IRKRNVFYQLSNLIS
ceHID-1	534	TDAAASAKRTLSCKKS	-----TPEL	SRTSGSEGTSMGSRPAAAEAP
dmHID-1	553	TDMAASAKRTLSCKKSGKTKGKFNLRVPRQRT	PAYSQELPSARVPEE	NEDEDEDEE
hhID-1	569	TDPPTEHKAQKRRR	-----	
ceHID-1	573	AADAPAAQTLGCVSTTTG	-----	LAATPALASMTGNVGNWEERESSQDNEM
dmHID-1	648	GTLKTSLLDTPCTQMTEREQAHPNDKQVEDS	TDIVYDRSAASTPDERKST	SPTLSRLSVARRASIRRVPGESDRM
hhID-1	611	GTLKTSLVATPCGLDKL	TENSQVSEDC	-----TLRSLEPEPQQSLEDGSPAKCEP
ceHID-1	635	LQTIMRLQLVLPQVEKICIDKGLDDESEIL	FLQHGTLVGLLVPVPHIVIRRYQ	TNIGTNHMFRTMMGVLYLKHQTP
dmHID-1	743	LQTIMRLQLVLPQVEKICIDKGLDDESEIL	FLQHGTLVGLLVPVPHIVIRRYQ	TNIGTNHMFRTMMGVLYLKHQTP
hhID-1	694	LQTIMRLQLVLPQVEKICIDKGLDDESEIL	FLQHGTLVGLLVPVPHIVIRRYQ	TNIGTNHMFRTMMGVLYLKHQTP

D->V sa1056

G->E sa1058

tion of a secondary signal (APFELD and KENYON 1998). New mutants that we isolated may define genes in this secondary pathway.

In addition to *pdk-1* and *akt-1*, our screen isolated mutations in the genes *aex-6*, *hid-1*, and *hid-2*, which, on the basis of strong suppression by *daf-16* and weak suppression by *daf-5*, also appear to act in the insulin branch of the pathway. In addition to their similar dauer phenotypes, *aex-6* and *hid-1* have similar defecation and locomotion phenotypes. Thus, these two genes may function together in a common process to regulate dauer formation, defecation, and locomotion. *aex-6* has the more severe defecation defect, while *hid-1* has the more severe movement defect. The pleiotropic phenotypes of these genes suggest a neuronal site of action, and *hid-1* is expressed primarily in neurons. The molecular identity of HID-1 as a putative multipass transmembrane protein suggests several possible functions. First, it could be involved in vesicle secretion. Like UNC-64 and UNC-31, HID-1 could regulate vesicle fusion with the plasma membrane, or it could be involved in vesicle sorting and secretion at an earlier step. Second, HID-1 could be a receptor for an intercellular signal, such as the proposed secondary signal activated by DAF-2 signaling. It is also possible that HID-1 itself acts as a novel insulin receptor. *daf-2* encodes the only classical insulin receptor in the *C. elegans* genome and evidence exists for additional insulin receptors (PIERCE *et al.* 2001). There is a HID-1 relative in *Schizosaccharomyces pombe* (but not *Saccharomyces cerevisiae*) with ~20% identity across nearly the entire length of HID-1, possibly supporting a vesicle secretion role. ESTs for the human and mouse HID-1 homologs were found in such tissues as brain, retina, hippocampus, and pancreatic islet cells, consistent with a neurosecretory function.

hid-1 and *aex-6* also exhibit a novel interaction with the *akt-1(mg144gf)* gain-of-function mutation. Double mutants of *hid-1* and *aex-6* with *akt-1(mg144gf)* produce some normal dauers, some partial dauers, and some non-dauers. *daf-16* mutants form similar partial dauers, but never produce normal dauers. It has been proposed that *daf-16* has roles in regulating both the decision to form a dauer and certain aspects of dauer morphogenesis (VOWELS and THOMAS 1992; GOTTLIEB and RUVKUN 1994; OGG *et al.* 1997). How can the formation of both complete and partial dauers by *akt-1(mg144gf)* be explained? One possibility is that formation of partial dauers is not due to specific defects in morphogenesis, but is due to differences in dauer induction based on quantitative input from various branches in the pathway. In *daf-16* mutants, which completely block input from the insulin branch, partial dauer formation may result when other pathway inputs are sufficient to induce a dauer. *akt-1(mg144gf)* may reduce *daf-16* activity to intermediate levels capable of inducing either normal or partial dauers. This raises the possibility that there are conditions under which the wild type forms partial

dauers. Why would wild-type animals deliberately make a partial dauer? Partial dauers of the type seen here are radially constricted and have modifications of the cuticle, like normal dauers. The main visible differences are that the partial dauers do not have a dark intestine (evidence of fat storage) and do not remodel their pharynx. Perhaps such partial dauers are formed when a modified cuticle is desirable to resist harsh environmental conditions, but when the animal has not been able to store enough fat. Under these conditions it would be desirable to remain capable of feeding, hence the unmodified pharynx. If the insulin signal monitors internal energy stores, as has been proposed on the basis of the actions of mammalian insulin (KIMURA *et al.* 1997), levels of signaling from this pathway could couple metabolic needs to morphological changes. Since other mutants in the insulin branch of the pathway can also form arrested dauer-like animals that have dark intestines but are not radially constricted, there may be multiple ways the insulin signal regulates dauer morphology. We speculate that wild-type *C. elegans* can form several different types of dauer-like animals that are adaptive under different combinations of environmental conditions and internal metabolic states. Perhaps these different types of dauers are formed frequently only under conditions that are not commonly experienced in our limited laboratory setting.

The 27° screen does not find mutants only in the insulin branch of the pathway. We isolated alleles of *unc-3* and *cam-1*, which appear to function in the group II Daf-c branch (KOGA *et al.* 1999; AILION and THOMAS 2000), and alleles of *tax-4*, which may function in upstream chemosensory signal transduction in both the group I and group II pathways (COBURN *et al.* 1998; AILION and THOMAS 2000). Thus, the continued analysis of mutants isolated in this screen is likely to be highly informative to understanding the complex molecular mechanisms responsible for regulating dauer formation.

We thank Makoto Koga, Chris Li, Gert Jansen, Oliver Hobert, and Gary Ruvkun for strains; Makoto Koga for the *cam-1(+)* clone; Scott Kennedy and Gary Ruvkun for *akt-1* primers; Yuji Kohara for cDNA clones; Alan Coulson for cosmids; Andy Fire for GFP vectors; Gemma Brown for editing; and Josh McElwee for heavy lifting. Some strains were provided by the *Caenorhabditis* Genetics Center, which is funded by the National Institutes of Health National Center for Research Resources. This work was supported by a Howard Hughes Medical Institute Predoctoral Fellowship to M.A. and National Institutes of Health grant R01GM48700 to J.H.T.

LITERATURE CITED

- AILION, M., and J. H. THOMAS, 2000 Dauer formation induced by high temperatures in *Caenorhabditis elegans*. *Genetics* **156**: 1047–1067.
- AILION, M., T. INOUE, C. I. WEAVER, R. W. HOLDCRAFT and J. H. THOMAS, 1999 Neurosecretory control of aging in *Caenorhabditis elegans*. *Proc. Natl. Acad. Sci. USA* **96**: 7394–7397.
- ANN, K., J. A. KOWALCHYK, K. M. LOYET and T. F. J. MARTIN, 1997 Novel Ca²⁺-binding protein (CAPS) related to UNC-31 required for Ca²⁺-activated exocytosis. *J. Biol. Chem.* **272**: 19637–19640.

- APFELD, J., and C. KENYON, 1998 Cell nonautonomy of *C. elegans* *daf-2* function in the regulation of diapause and life span. *Cell* **95**: 199–210.
- AVERY, L., 1993 The genetics of feeding in *Caenorhabditis elegans*. *Genetics* **133**: 897–917.
- BIRNBY, D. A., E. M. LINK, J. J. VOWELS, H. TIAN, P. L. COLACURCIO *et al.*, 2000 A transmembrane guanylyl cyclase (DAF-11) and Hsp90 (DAF-21) regulate a common set of chemosensory behaviors in *Caenorhabditis elegans*. *Genetics* **155**: 85–104.
- BRENNER, S., 1974 The genetics of *Caenorhabditis elegans*. *Genetics* **77**: 71–94.
- CASSADA, R. C., and R. L. RUSSELL, 1975 The dauerlarva, a post-embryonic developmental variant of the nematode *Caenorhabditis elegans*. *Dev. Biol.* **46**: 326–342.
- COBURN, C. M., and C. I. BARGMANN, 1996 A putative cyclic nucleotide-gated channel is required for sensory development and function in *C. elegans*. *Neuron* **17**: 695–706.
- COBURN, C. M., I. MORI, Y. OHSHIMA and C. I. BARGMANN, 1998 A cyclic nucleotide-gated channel inhibits sensory axon outgrowth in larval and adult *Caenorhabditis elegans*: a distinct pathway for maintenance of sensory axon structure. *Development* **125**: 249–258.
- DANIELS, S. A., M. AILION, J. H. THOMAS and P. SENGUPTA, 2000 *egl-4* acts through a transforming growth factor- β /SMAD pathway in *Caenorhabditis elegans* to regulate multiple neuronal circuits in response to sensory cues. *Genetics* **156**: 123–141.
- ESTEVEZ, M., L. ATTISANO, J. L. WRANA, P. S. ALBERT, J. MASSAGUÉ *et al.*, 1993 The *daf-4* gene encodes a bone morphogenetic protein receptor controlling *C. elegans* dauer larva development. *Nature* **365**: 644–649.
- FORRESTER, W. C., E. PERENS, J. A. ZALLEN and G. GARRIGA, 1998 Identification of *Caenorhabditis elegans* genes required for neuronal differentiation and migration. *Genetics* **148**: 151–165.
- FORRESTER, W. C., M. DELL, E. PERENS and G. GARRIGA, 1999 A *C. elegans* Ror receptor tyrosine kinase regulates cell motility and asymmetric cell division. *Nature* **400**: 881–885.
- GEORGI, L. L., P. S. ALBERT and D. L. RIDDLE, 1990 *daf-1*, a *C. elegans* gene controlling dauer larva development, encodes a novel receptor protein kinase. *Cell* **61**: 635–645.
- GOLDEN, J. W., and D. L. RIDDLE, 1984a The *Caenorhabditis elegans* dauer larva: developmental effects of pheromone, food, and temperature. *Dev. Biol.* **102**: 368–378.
- GOLDEN, J. W., and D. L. RIDDLE, 1984b A pheromone-induced developmental switch in *Caenorhabditis elegans*: temperature-sensitive mutants reveal a wild-type temperature-dependent process. *Proc. Natl. Acad. Sci. USA* **81**: 819–823.
- GOLDEN, J. W., and D. L. RIDDLE, 1984c A *Caenorhabditis elegans* dauer-inducing pheromone and an antagonistic component of the food supply. *J. Chem. Ecol.* **10**: 1265–1280.
- GOTTLIEB, S., and G. RUVKUN, 1994 *daf-2*, *daf-16* and *daf-23*: genetically interacting genes controlling dauer formation in *Caenorhabditis elegans*. *Genetics* **137**: 107–120.
- HEDGECOCK, E. M., J. G. CULOTTI, J. N. THOMSON and L. A. PERKINS, 1985 Axonal guidance mutants of *Caenorhabditis elegans* identified by filling sensory neurons with fluorescein dyes. *Dev. Biol.* **111**: 158–170.
- HIROSE, T., Y. NAKANO, Y. NAGAMATSU, T. MISUMI, H. OHTA *et al.*, 2003 Cyclic GMP-dependent protein kinase EGL-4 controls body size and lifespan in *C. elegans*. *Development* **130**: 1089–1099.
- HUANG, L. S., P. TZOU and P. W. STERNBERG, 1994 The *lin-15* locus encodes two negative regulators of *Caenorhabditis elegans* vulval development. *Mol. Biol. Cell* **5**: 395–411.
- INOUE, T., and J. H. THOMAS, 2000a Targets of TGF- β signaling in *Caenorhabditis elegans* dauer formation. *Dev. Biol.* **217**: 192–204.
- INOUE, T., and J. H. THOMAS, 2000b Suppressors of transforming growth factor- β pathway mutants in the *Caenorhabditis elegans* dauer formation pathway. *Genetics* **156**: 1035–1046.
- IWASAKI, K., D. W. C. LIU and J. H. THOMAS, 1995 Genes that control a temperature-compensated ultradian clock in *Caenorhabditis elegans*. *Proc. Natl. Acad. Sci. USA* **92**: 10317–10321.
- IWASAKI, K., J. STAUNTON, O. SAIFEE, M. NONET and J. H. THOMAS, 1997 *aex-3* encodes a novel regulator of presynaptic activity in *C. elegans*. *Neuron* **18**: 613–622.
- KATSURA, I., K. KONDO, T. AMANO, T. ISHIHARA and M. KAWAKAMI, 1994 Isolation, characterization and epistasis of fluoride-resistant mutants of *Caenorhabditis elegans*. *Genetics* **136**: 145–154.
- KIMURA, K. D., H. A. TISSENBAUM, Y. LIU and G. RUVKUN, 1997 *daf-2*, an insulin receptor-like gene that regulates longevity and diapause in *Caenorhabditis elegans*. *Science* **277**: 942–946.
- KOGA, M., M. TAKEUCHI, T. TAMEISHI and Y. OHSHIMA, 1999 Control of DAF-7 TGF- β expression and neuronal process development by a receptor tyrosine kinase KIN-8 in *Caenorhabditis elegans*. *Development* **126**: 5387–5398.
- KOMATSU, H., I. MORI, J.-S. RHEE, N. AKAIKE and Y. OHSHIMA, 1996 Mutations in a cyclic nucleotide-gated channel lead to abnormal thermosensation and chemosensation in *C. elegans*. *Neuron* **17**: 707–718.
- LIN, K., J. B. DORMAN, A. RODAN and C. KENYON, 1997 *daf-16*: an HNF-3/forkhead family member that can function to double the life-span of *Caenorhabditis elegans*. *Science* **278**: 1319–1322.
- LIVINGSTONE, D., 1991 Studies on the *unc-31* gene of *Caenorhabditis elegans*. Ph.D. Thesis, University of Cambridge, Cambridge, UK.
- MALONE, E. A., and J. H. THOMAS, 1994 A screen for nonconditional dauer-constitutive mutations in *Caenorhabditis elegans*. *Genetics* **136**: 879–886.
- MALONE, E. A., T. INOUE and J. H. THOMAS, 1996 Genetic analysis of the roles of *daf-28* and *age-1* in regulating *Caenorhabditis elegans* dauer formation. *Genetics* **143**: 1193–1205.
- MELLO, C. C., J. M. KRAMER, D. STINCHCOMB and V. AMBROS, 1991 Efficient gene transfer in *C. elegans*: extrachromosomal maintenance and integration of transforming sequences. *EMBO J.* **10**: 3959–3970.
- MORRIS, J. Z., H. A. TISSENBAUM and G. RUVKUN, 1996 A phosphatidylinositol-3-OH kinase family member regulating longevity and diapause in *Caenorhabditis elegans*. *Nature* **382**: 536–539.
- NELSON, L. S., M. L. ROSOFF and C. LI, 1998 Disruption of a neuropeptide gene, *flp-1*, causes multiple behavioral defects in *Caenorhabditis elegans*. *Science* **281**: 1686–1690.
- OGAWA, H., S. HARADA, T. SASSA, H. YAMAMOTO and R. HOSONO, 1998 Functional properties of the *unc-64* gene encoding a *Caenorhabditis elegans* syntaxin. *J. Biol. Chem.* **273**: 2192–2198.
- OGG, S., S. PARADIS, S. GOTTLIEB, G. I. PATTERSON, L. LEE *et al.*, 1997 The Fork head transcription factor DAF-16 transduces insulin-like metabolic and longevity signals in *C. elegans*. *Nature* **389**: 994–999.
- PARADIS, S., and G. RUVKUN, 1998 *Caenorhabditis elegans* Akt/PKB transduces insulin receptor-like signals from AGE-1 PI3 kinase to the DAF-16 transcription factor. *Genes Dev.* **12**: 2488–2498.
- PARADIS, S., M. AILION, A. TOKER, J. H. THOMAS and G. RUVKUN, 1999 A PDK1 homolog is necessary and sufficient to transduce AGE-1 PI3 kinase signals that regulate diapause in *Caenorhabditis elegans*. *Genes Dev.* **13**: 1438–1452.
- PATTERSON, G. I., A. KOWEEK, A. WONG, Y. LIU and G. RUVKUN, 1997 The DAF-3 Smad protein antagonizes TGF- β -related receptor signaling in the *Caenorhabditis elegans* dauer pathway. *Genes Dev.* **11**: 2679–2690.
- PIERCE, S. B., M. COSTA, R. WISOTZKEY, S. DEVADHAR, S. A. HOMBURGER *et al.*, 2001 Regulation of DAF-2 receptor signaling by human insulin and *ins-1*, a member of the unusually large and diverse *C. elegans* insulin gene family. *Genes Dev.* **15**: 672–686.
- PRASAD, B. C., B. YE, R. ZACKHARY, K. SCHRADER, G. SEYDOUX *et al.*, 1998 *unc-3*, a gene required for axonal guidance in *Caenorhabditis elegans*, encodes a member of the O/E family of transcription factors. *Development* **125**: 1561–1568.
- QIN, H., J. L. ROSENBAUM and M. M. BARR, 2001 An autosomal recessive polycystic kidney disease gene homolog is involved in intraflagellar transport in *C. elegans* ciliated sensory neurons. *Curr. Biol.* **11**: 457–461.
- REN, P., C.-S. LIM, R. JOHNSEN, P. S. ALBERT, D. PILGRIM *et al.*, 1996 Control of *C. elegans* larval development by neuronal expression of a TGF- β homolog. *Science* **274**: 1389–1391.
- RIDDLE, D. L., and P. S. ALBERT, 1997 Genetic and environmental regulation of dauer larva development, pp. 739–768 in *C. elegans II*, edited by D. L. RIDDLE, T. BLUMENTHAL, B. J. MEYER and J. R. PRIESS. Cold Spring Harbor Laboratory Press, Cold Spring Harbor, NY.
- SAIFEE, O., L. WEI and M. NONET, 1998 The *Caenorhabditis elegans* *unc-64* locus encodes a syntaxin that interacts genetically with synaptobrevin. *Mol. Biol. Cell* **9**: 1235–1252.
- SCHACKWITZ, W. S., 1996 Genetic and neural processing of the dauer

- pheromone response in *Caenorhabditis elegans*. Ph.D. Thesis, University of Washington, Seattle.
- SCHACKWITZ, W. S., T. INOUE and J. H. THOMAS, 1996 Chemosensory neurons function in parallel to mediate a pheromone response in *C. elegans*. *Neuron* **17**: 719–728.
- STARICH, T. A., R. K. HERMAN, C. K. KARI, W.-H. YEH, W. S. SCHACKWITZ *et al.*, 1995 Mutations affecting the chemosensory neurons of *Caenorhabditis elegans*. *Genetics* **139**: 171–188.
- SZE, J. Y., M. VICTOR, C. LOER, Y. SHI and G. RUVKUN, 2000 Food and metabolic signaling defects in a *Caenorhabditis elegans* serotonin-synthesis mutant. *Nature* **403**: 560–564.
- TAKE-UCHI, M., M. KAWAKAMI, T. ISHIHARA, T. AMANO, K. KONDO *et al.*, 1998 An ion channel of the degenerin/epithelial sodium channel superfamily controls the defecation rhythm in *Caenorhabditis elegans*. *Proc. Natl. Acad. Sci. USA* **95**: 11775–11780.
- THOMAS, J. H., 1990 Genetic analysis of defecation in *Caenorhabditis elegans*. *Genetics* **124**: 855–872.
- THOMAS, J. H., D. A. BIRNBY and J. J. VOWELS, 1993 Evidence for parallel processing of sensory information controlling dauer formation in *Caenorhabditis elegans*. *Genetics* **134**: 1105–1117.
- TOKER, A., and L. C. CANTLEY, 1997 Signaling through the lipid products of phosphoinositide-3-OH kinase. *Nature* **387**: 673–676.
- VOWELS, J. J., and J. H. THOMAS, 1992 Genetic analysis of chemosensory control of dauer formation in *Caenorhabditis elegans*. *Genetics* **130**: 105–123.
- VOWELS, J. J., and J. H. THOMAS, 1994 Multiple chemosensory defects in *daf-11* and *daf-21* mutants of *Caenorhabditis elegans*. *Genetics* **138**: 303–316.
- WOLKOW, C. A., K. D. KIMURA, M.-S. LEE and G. RUVKUN, 2000 Regulation of *C. elegans* life-span by insulin-like signaling in the nervous system. *Science* **290**: 147–150.
- ZHAO, C., and S. W. EMMONS, 1995 A transcription factor controlling development of peripheral sense organs in *C. elegans*. *Nature* **373**: 74–77.
- ZWAAL, R. R., J. E. MENDEL, P. W. STERNBERG and R. H. A. PLASTERK, 1997 Two neuronal G proteins are involved in chemosensation of the *Caenorhabditis elegans* dauer-inducing pheromone. *Genetics* **145**: 715–727.

Communicating editor: P. ANDERSON